Biochemical and Biophysical Research Communications 400 (2010) 27–33

Contents lists available at ScienceDirect

Biochemical and Biophysical Research Communications

journal homepage: www.elsevier.com/locate/ybbrc

Neonatal mouse testis-derived multipotent germline stem cells improve the cardiac function of acute ischemic heart mouse model

Toru Iwasa [a], Shiro Baba [a,*], Hiraku Doi [a], Shinji Kaichi [a], Noritaka Yokoo [a], Takahiro Mima [a], Mito Kanatsu-Shinohara [b], Takashi Shinohara [b,1], Tatsutoshi Nakahata [a], Toshio Heike [a]

[a] Department of Pediatrics, Graduate School of Medicine, Kyoto University, 54 Kawahara-cho, Shogoin, Sakyo-ku, Kyoto 606-8507, Japan
[b] Department of Molecular Genetics, Graduate School of Medicine, Kyoto University, Konoe-cho, Yoshida Sakyo-ku, Kyoto 606-8501, Japan

ARTICLE INFO

Article history:
Received 29 July 2010
Available online 4 August 2010

Keywords:
mGS
Flk1
Cardiac regeneration therapy

ABSTRACT

Multipotent germline stem (mGS) cells have been established from neonatal mouse testes. We previously reported that undifferentiated mGS cells are phenotypically similar to embryonic stem cells and that fetal liver kinase 1 (Flk1)$^+$ mGS cells have a similar potential to differentiate into cardiomyocytes and endothelial cells compared with Flk1$^+$ embryonic stem cells. Here, we transplanted these Flk1$^+$ mGS cells into an ischemic heart failure mouse model to evaluate the improvement in cardiac function. Significant increase in left ventricular wall thickness of the infarct area, left ventricular ejection fraction and left ventricular maximum systolic velocity was observed 4 weeks after when sorted Flk1$^+$ mGS cells were transplanted directly into the hearts of the acute ischemic model mice. Although the number of cardiomyocytes derived from Flk1$^+$ mGS cells were too small to account for the improvement in cardiac function but angiogenesis around ischemic area was enhanced in the Flk1$^+$ mGS cells transplanted group than the control group and senescence was also remarkably diminished in the early phase of ischemia according to β-galactosidase staining assay. In conclusion, Flk1$^+$ mGS cell transplantation can improve the cardiac function of ischemic hearts by promoting angiogenesis and by delaying host cell death via senescence.

1. Introduction

The main cause of severe heart failure is ischemic heart disease. Although heart transplantation is the most effective therapy for end-stage severe heart failure, demand of donor hearts far outstrips supply of available hearts [1]. To this end, cardiac stem/progenitor cells are considered as one of promising source for radical cell-based therapies to bridge ischemic heart disease patients to or altogether replace heart transplantation [2–6].

Several studies reported that embryonic stem (ES) cells are one of hopeful cell source for transplantation into heart and improvement of cardiac function had observed by the transplantation of ES cells. Because ES cell are derived from fertilized eggs, there is ethical problem in establishment of human ES cells and application for human therapy. Furthermore ES cells are derived from other individuals, there is also immunological problem of host rejection to the transplanted cells.

Recently multipotent germline stem (mGS) cells were established from neonatal mouse testis. The mGS cells have less ethical problem compared with ES cells and if the mGS cells are established from an ischemic heart disease patient and the mGS cells are applied for treatment of the patient, we can provide novel and better cell therapy for ischemic heart disease with less ethical and immunological problem.

We previously reported that mGS cells from neonatal mouse testis are as favorable as mouse ES cells for differentiation into cardiomyocytes and endothelial cells by the selection with the mesodermal cell surface marker [7,8], fetal liver kinase 1 (Flk1) [9,10]. The differentiated cardiomyocytes derived from mGS cells have similar electrophysiology as adult mouse cardiomyocytes *in vitro* [10]. Furthermore, we reported that Flk1$^+$ cells derived from ES cells have the potential to improve cardiac function in a model of cardiomyopathy by direct cardiac transplantation [5]. Given these convincing results, we transplanted Flk1$^+$ cells derived from mGS cells directly into acute ischemic hearts, and evaluated the improvement in cardiac function. Moreover, we studied the effect of Flk1$^+$ mGS cell-transplantation on cardiac regeneration.

Abbreviations: mGS cells, multipotent germline stem cells; Flk1, fetal liver kinase 1; ES cells, embryonic stem cells; FCS, fetal calf serum; 2ME, 2-mercaptoethanol; LIF, leukemia inhibitory factor; LAD, left anterior descendant coronary artery; LVDd, left ventricular end-diastolic diameter; LVEF, left ventricular ejection fraction; +dP/dt, maximum systolic velocity change; −dP/dt, minimum diastolic velocity change; cTn-I, cardiac troponin-I; TUNEL, terminal deoxynucleotidyl transferase dUTP nick end labeling; AMI, acute myocardial infarct; iPS cells, induced pluripotent stem cells.

* Corresponding author. Fax: +81 75 752 2361.
E-mail addresses: shibaba@kuhp.kyoto-u.ac.jp (S. Baba), tshinoha@virus.kyoto-u.ac.jp (T. Shinohara).
[1] Fax: +81 75 751 4169.

0006-291X/$ - see front matter © 2010 Elsevier Inc. All rights reserved.
doi:10.1016/j.bbrc.2010.07.131

2. Materials and methods

2.1. Cell culture and differentiation

Green fluorescence protein positive mGS cells were maintained on mouse embryonic fibroblasts in DMEM (Sigma) containing 15% fetal calf serum (FCS) (Sigma), 1×10^{-4} M 2-mercaptoethanol (2ME) and 5000 U/ml leukemia inhibitory factor (LIF) as described previously [9,10]. These cells were differentiated into mesodermal cells on OP-9 stromal cell layers in alpha-MEM (Gibco) containing 10% FCS (Sigma) and 5×10^{-5} M 2ME without LIF (differentiation medium) at a concentration of 3×10^4 cells/25 cm^2 flask (FALCON) [10,11]. OP-9 cell line was a kind gift from Dr. Kodama and was maintained as described previously [12].

2.2. FACS Vantage sorting

The cell surface marker antibodies used in these FACS experiments were a rat anti-mouse Flk1 antibody (BD Pharmingen) [7] and allophycocyanin-conjugated anti-rat IgG antibody served as a secondary antibody. Analysis was performed by FACSCalibur (BD Biosciences). The mGS cell derivatives were divided into $Flk1^+$ and $Flk1^-$ cells by anti-Flk1 labeling followed by sorting with a FACSVantage SE (BD Biosciences) 4 days after differentiation.

2.3. β-Galactosidase assay

Cell-transplanted hearts were removed quickly on day 3 and day 7 after the cells transplantation, each heart coronal sections were incubated at 37 °C (no CO_2) with fresh senescence-associated β-galactosidase (3-Gal (SA-3-Gal) stain solution: 1 mg of 5-bromo-4-chloro-3-indolyl P3-D-galactoside (X-Gal) per ml/40 mM citric acid/sodium phosphate, pH 6.0/5 mM potassium ferrocyanide/5 mM potassium ferrocyanide/150 mM NaCl/2 mM $MgCl_2$ [13,14]. Staining was evident in 2–4 h and all the specimens were incubated for 6 h.

2.4. Transplantation of mGS cells to acute myocardial ischemic model mice

To produce acute myocardial ischemic model mice, we used 8-week-old male DBA/2 mice. As mGS cells were produced from these DBA/2 mice testes, the MHC types of this mouse and mGS cells are same. All animal handling procedures followed the Guide for the Care and Use of Laboratory Animals published by the US National Institutes of Health (NIH Publication No. 85–23, revised 1996) and the guidelines of the Animal Research Committee of the Graduate School of Medicine, Kyoto University. Mice were anesthetized and intubated for mechanical controlled ventilation before thoracotomy. After opening their left intercostal space, left anterior descendant coronary artery (LAD) was ligated permanently. The 10 μl of $Flk1^+$ or $Flk1^-$ mGS cells suspension (3×10^5/10 μl) was then injected dividedly into two sites of marginal zone (between scar area and normal area). The number of mice were as follows, $n = 10$ for $Flk1^+$ mGS cells transplantation, $n = 5$ for $Flk1^-$ mGS cells transplantation, $n = 14$ for medium injection (sham group), $n = 10$ for non-treatment (control group).

2.5. Hemodynamic measurements and electrocardiogram recordings

Hemodynamics was indirectly measured via echocardiography with a 15–16 MHz phased-array transducer (model 21390A, PHILIPS). Left ventricular diastolic diameter (LVDd) and left ventricular systolic diameter were measured and the left ventricular ejection fraction (LVEF) was calculated as previously described [2]. Cardiac catheterization was performed 4 weeks after the cell transplantation by using a 1.4-Fr micro manometer tipped catheter (Miller Instruments Inc.). Left ventricular pressure curve was recorded and left ventricular maximum systolic velocity (+dP/dt) and minimum diastolic velocity (−dP/dt) were calculated by a PowerLab System (PowerLab 4/25 ML845 and BIO Amp CF ML132) (ADInstruments) [5]. All measurements were performed under anesthesia with mask inhalation of 0.5–1.0% sevoflurane and a heart rate of approximately 450/min.

2.6. Histology

Tissue slices (7 μm) were fixed with 4% paraformaldehyde and incubated with antibodies specific for the following markers: cardiac troponin-I (cTn-I) (Santa Cruz Biotechnology), CD31 (Becton Dickinson), p53 (BD Pharmingen) and p21 (BD Pharmingen). Cy3-conjugated donkey anti-mouse IgG, Cy3-conjugated donkey anti-goat IgG, and Cy3-conjugated goat anti-rat IgG (Jackson ImmunoResearch Laboratories, Inc.) served as secondary antibodies. All heart sections were incubated with these antibodies using the M.O.M. kit (Vector Laboratories, Inc.) to prevent non-specific reactions. Many heart slices were also stained with hematoxylin–eosin (HE) to detect abnormal cell growth due to transplanted $Flk1^+$ or $Flk1^-$ mGS cells. Hearts fixed in 10% formalin were embedded in paraffin, sectioned at 4 μm thickness, and stained with Masson-Trichrome for detecting fibrosis in infarcted areas. For apoptosis analysis, infarcted hearts were frozen in cryomolds, sectioned, and terminal deoxynucleotidyl transferase dUTP nick end labeling (TUNEL) was performed according to the manufacturer's protocol (*In Situ* Apoptosis Detection kit; Takara).

2.7. Statistical analysis

Data were analyzed with paired or unpaired two-tail Student's *t*-test with Microsoft Excel software. Statistical significance was defined as a p value of less than 0.05.

3. Results

3.1. Transplantation of $Flk1^+$ mGS cells significantly improves the cardiac function of ischemic hearts

We used 8-week-old male DBA/2 mice. Ten minutes after permanent LAD occlusion, 3×10^5 $Flk1^+$ mGS cells were transplanted equally into two sites of the anterior left ventricular free wall. As a control group, an equivalent volume of medium was injected into the AMI model mouse hearts in a similar fashion.

To investigate whether $Flk1^+$ mGS cells undergo cardiomyogenesis *in vivo* as efficiently as they do *in vitro* and whether cardiac function improves after $Flk1^+$ mGS cell transplantation, we sorted mGS-derived $Flk1^+$ cells on day 4 of differentiation (Fig. 1A). A total of 39 mice were used in these experiments as follows: 10 AMI model mice were transplanted with $Flk1^+$ mGS cells, 14 AMI model mice were injected with an equivalent volume of medium alone, and 10 normal mice were used as controls. In addition, we injected $Flk1^-$ mGS cells into hearts of 5 AMI model mice. To assess the severity of cardiomyopathy in the AMI model mice, LVDd and LVEF were assessed by echocardiography at weeks 0 and 4. Although the LVDd of the $Flk1^+$ mGS cell transplanted group and the medium injected group was not significantly different at 4 weeks after the cell transplantation, the $Flk1^+$ mGS cell transplanted group had significantly higher LVEF values than the medium injected group (Fig. 1B and C).

Cardiac catheterization in mice was used to evaluate the left ventricular +dP/dt and left ventricular −dP/dt parameters at 4 weeks

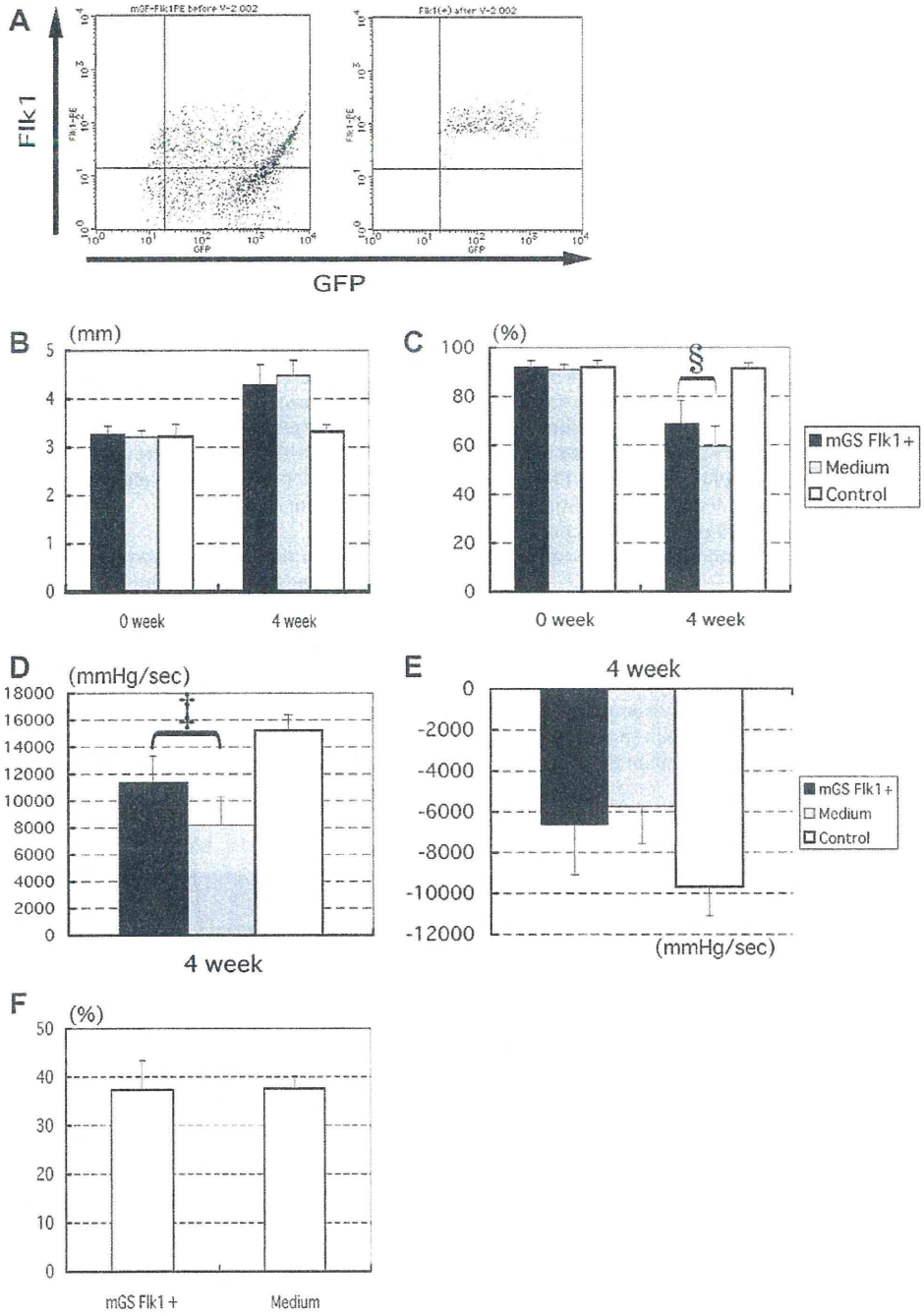

Fig. 1. (A) mGS cell-derived Flk1$^+$ cells were detected clearly after 4-day differentiation (left panel). Flk1$^+$ mGS cells were sorted by flow cytometry with greater than 97% purity (right panel). (B,C) The results of echocardiography in each group. LVDd between in the Flk1$^+$ mGS cell transplanted group and in the medium injected control group was not significantly different (B). LVEF between the Flk1$^+$ mGS cell transplanted group and the medium injected group was significantly different (C). (D,E) The results of cardiac catheterization in each group reveals that significant increase of +dP/dt in the Flk1$^+$ mGS cell transplant group, but not in the medium injected group. (F) The percentage of infarcted circumference was calculated in each group. $^{\ddagger}p < 0.01$, $^{\S}p < 0.05$.

after the cell transplantation. The Flk1$^+$ mGS cell transplanted group showed significant improvement in +dP/dt values when compared to the values of the medium injected group (Fig. 1D). As for −dP/dt, there were no significant difference between these two groups (Fig. 1E). These results indicated that Flk1$^+$ mGS cell transplantation was influenced by the systolic function, not diastolic function, of AMI model mouse hearts. Of course, the size of infarcted area (the ratio of infarcted circumference to the entire heart circumference) was not significantly different in each group as evaluated by Masson-Trichrome stain (Fig. 1F). In contrast, the cardiac function of Flk1$^-$ mGS cell transplanted group was not recovered 4 weeks after transplantation assessed by echocardiography and cardiac catheterization (LVDd 4.31 ± 0.41 mm, LVEF 57.6 ± 11.6%, +dP/dt 9167.4 ± 1722.2 mmHg/s, −dP/dt −5958.1 ± 1311.7 mmHg/s, respectively).

3.2. Flk1$^+$ mGS cells differentiated into cardiomyocytes and endothelial cells in AMI model mice heart

Cardiomyogenesis of the transplanted Flk1$^+$ mGS cells in AMI model mouse hearts was evaluated by immunohiostochemistory. Transplanted Flk1$^+$ mGS cells differentiated not only into cTn-I positive cardiomyocytes in the infarcted area but also endothelial cells that form tube-like structures (Fig. 2A and B). These differentiated cardiomyocytes and endothelial cells may partly contribute to the improvement of cardiac function.

To investigate another mechanism of the observed improved cardiac function with Flk1$^+$ mGS cell transplantation, we quantified the number of vessels in the marginal zone. The marginal zone was defined as the area between infarcted area and normal (non-ischemic) area. The number of the vessels, defined as tube-like structures with CD31 positive cells, was significantly higher in the Flk1$^+$ mGS cell transplanted group than that of the medium injected group (Fig. 2C). These results suggested that enhanced angiogenesis in the marginal zone should supply better blood flow in the Flk1$^+$ mGS transplanted group than in the medium injected group. In the hearts transplanted Flk1 mGS cells, we could not detect differentiated cardiomyocytes and endothelial cells derived from Flk1 mGS cells.

3.3. Preserved LV wall thickness in the marginal zone by the Flk1$^+$ mGS cells transplantation

In infarcted areas, we observed increased cardiomyocyte survival in the Flk1$^+$ mGS cell transplanted group than the medium injected group (Fig. 3A–D). The wall thickness of infarcted area was much thicker in the Flk1$^+$ mGS cell transplanted group than in the medium injected group (Fig. 3E). In contrast, the wall thickness of infarcted area in the Flk1$^-$ mGS cell transplanted group was same as that of the medium injected group.

3.4. Apoptosis in the marginal zone was not suppressed by the Flk1$^+$ mGS cells transplantation

To investigate the mechanism of cardiomyocyte survival, we first counted the number of apoptotic cells in the marginal zone of each group 0, 6, 12, and 24 h and 4 weeks by TUNEL staining after Flk1$^+$ cell transplantation or medium injection (Fig. 3F–H). The number of apoptotic cells rapidly increased 6 h after infarction and then gradually decreased until 24 h. The ratio of apoptotic cells to non-apoptotic cells 24 h after Flk1$^+$ mGS cell transplantation was almost the same as during the time course from 0 h to 4 weeks after Flk1$^+$ cell transplantation or medium injection (Fig. 3I). These results revealed that the observed apoptosis after infarction was not suppressed by Flk1$^+$ mGS cell transplantation compared to medium injection.

3.5. Senescence in the marginal zone was prevented and delayed by the Flk1$^+$ mGS cells transplantation

Next, we investigated the association of Flk1$^+$ mGS cell transplantation and senescence, a type of cell death [13,15,16]. Senescent cells were detected by a β-galactosidase assay 3 and 7 days after the Flk1$^+$ mGS cell transplantation and the medium injection. Although there were no significant difference in β-galactosidase stained areas between the Flk1$^+$ mGS cell transplanted group and

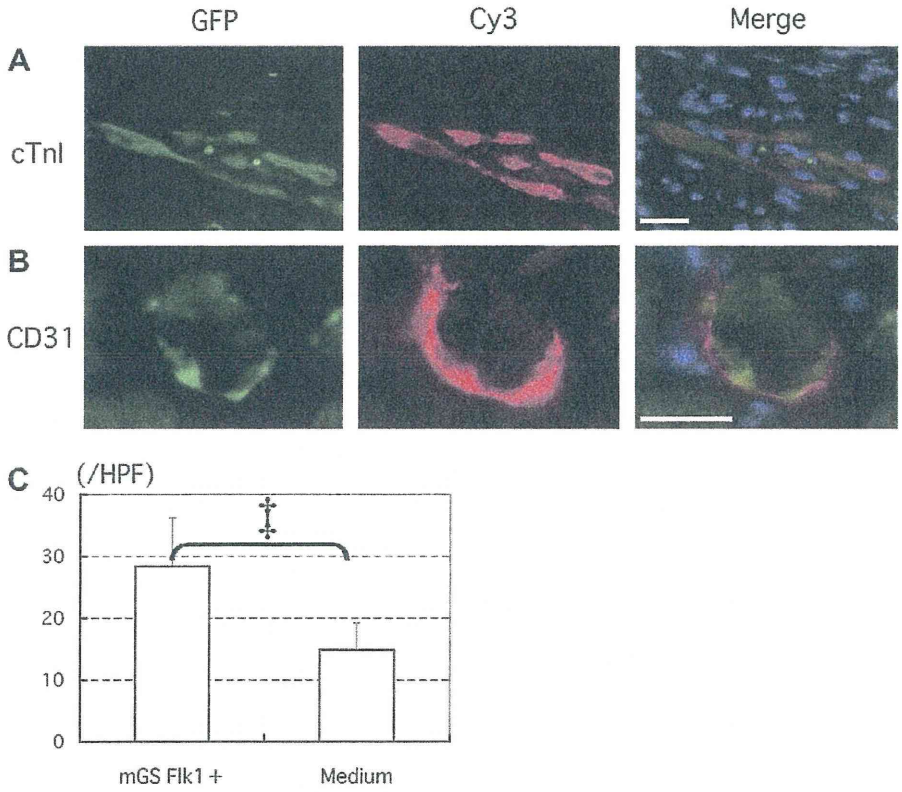

Fig. 2. (A) GFP$^+$ mGS cells (left, green) were stained with cardiac troponin-I (cTn-I) (middle, red). Merged image (right). (B) GFP$^+$ mGS cells with a tube structure (left panel, green) were stained with CD31 (middle panel, red). Merged image (right). The nuclei were counterstained with Hoechst 33342 (blue). (C) The number of CD31$^+$ vessels in the marginal zone in each group. Scale bar: 100 μm. $^1p < 0.01$. (For interpretation of the references to colour in this figure legend, the reader is referred to the web version of this article.)

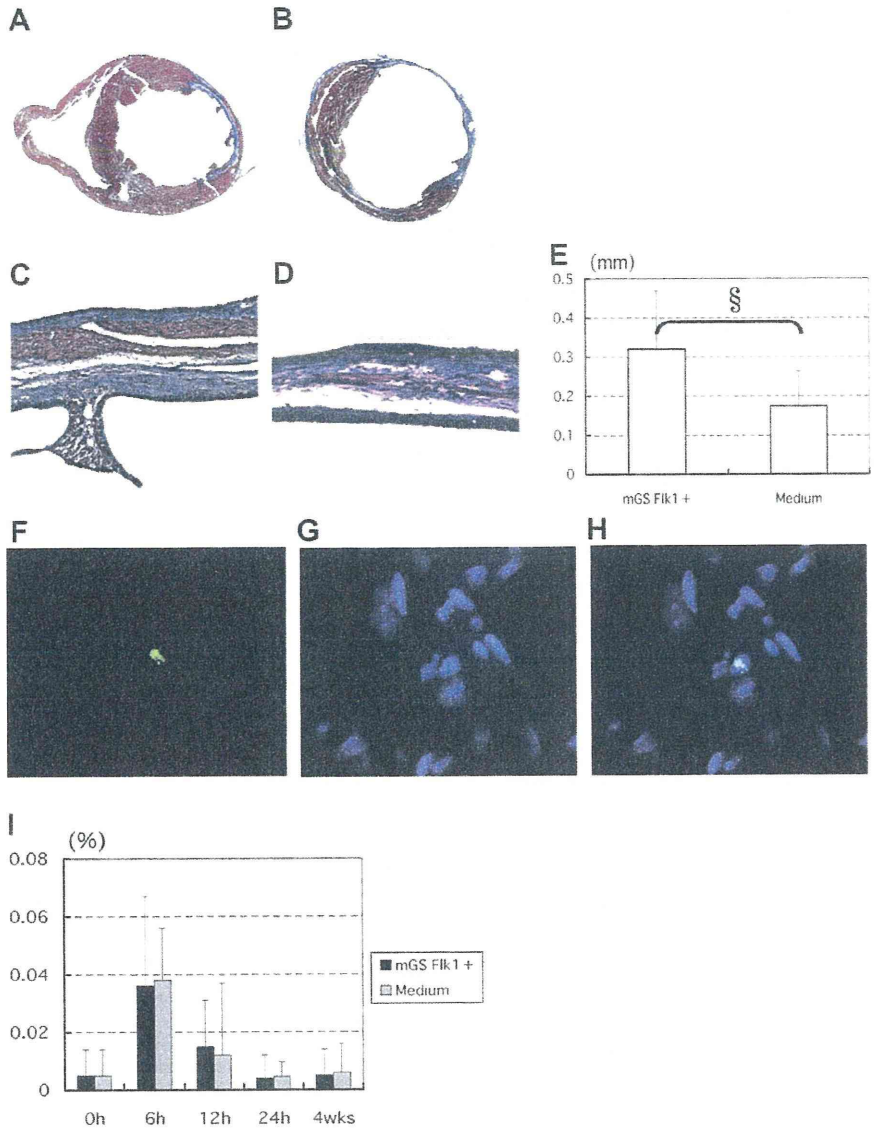

Fig. 3. (A) Coronal sections of Flk1$^+$ mGS cell transplanted heart 4 weeks after the cell transplantation. This section was stained with Masson-Trichrome stain. (C) A magnified area of infarcted area from panel A. (B) The coronal section of a medium injected heart 4 weeks after the injection. This section was stained with Masson-Trichrome stain. (D) The magnification of infarcted area in the panel B. (E) The thickness of the infarcted anterior wall in each group. $^{\S}p < 0.05$. (F–H) TUNEL positive nucleus (F: left, green) was detected in the marginal zone. The nuclei were counterstained with Hoechst 33342 (G: middle, blue). Merged image (H: right). (I) The percentages of TUNEL positive nuclei were compared after Flk1$^+$ mGS cell transplantation or control medium injection. There were no significant difference between the Flk1$^+$ mGS cell transplanted group and the medium injected group over the 4-week time course. (For interpretation of the references to colour in this figure legend, the reader is referred to the web version of this article.)

the medium injected group 7 days after the transplantation, the β-galactosidase stained area was undoubtedly smaller 3 days after the transplantation in the Flk1$^+$ mGS cell transplanted group than in the medium injection group (Fig. 4A–D). Especially in the Flk1$^+$ mGS cell transplanted group, the β-galactosidase stained area on days 3 was located in the endocardium side of infarcted area. On the other hand, the epicardium side of infarcted area was not stained deeply by the β-galactosidase (Fig. 4A). These results revealed that the cell dearth via the cell senescence was delayed by the Flk1$^+$ mGS cells transplantation. Finally, we investigated the cell signals, p21 and p53 that were elevated during the senescence pathway [17,18], to confirm that the senescence is actually prevented by the cells transplantation. Activated p21 and p53 were not clearly detected in the epicardium and endocardium sides of infarcted area in the Flk1$^+$ mGS cell transplanted group on 3 days after the cell transplantation (Fig. 4F and G). As to the medium injected group, activated p21 and p53 were clearly detected all layers from endocardium to epicardium in the infarcted area (Fig. 4H and I).

4. Discussion

There were a lot of candidates of cell sources for the cell transplantation to heart failure model animals [2–4,19–21]. In these sources, we reported the Flk1$^+$ mGS cells were one of the most convincing cell sources previously [10]. These Flk1$^+$ mGS cells have enough potential in their expansion at the undifferentiated state and in their differentiation into cardiomyocytes and endothelial cells *in vitro*. Under this knowledge, we transplanted these cells into the hearts of AMI model mice. Stem cells derived from various tissues including adipose tissue and bone marrow can also differenti-

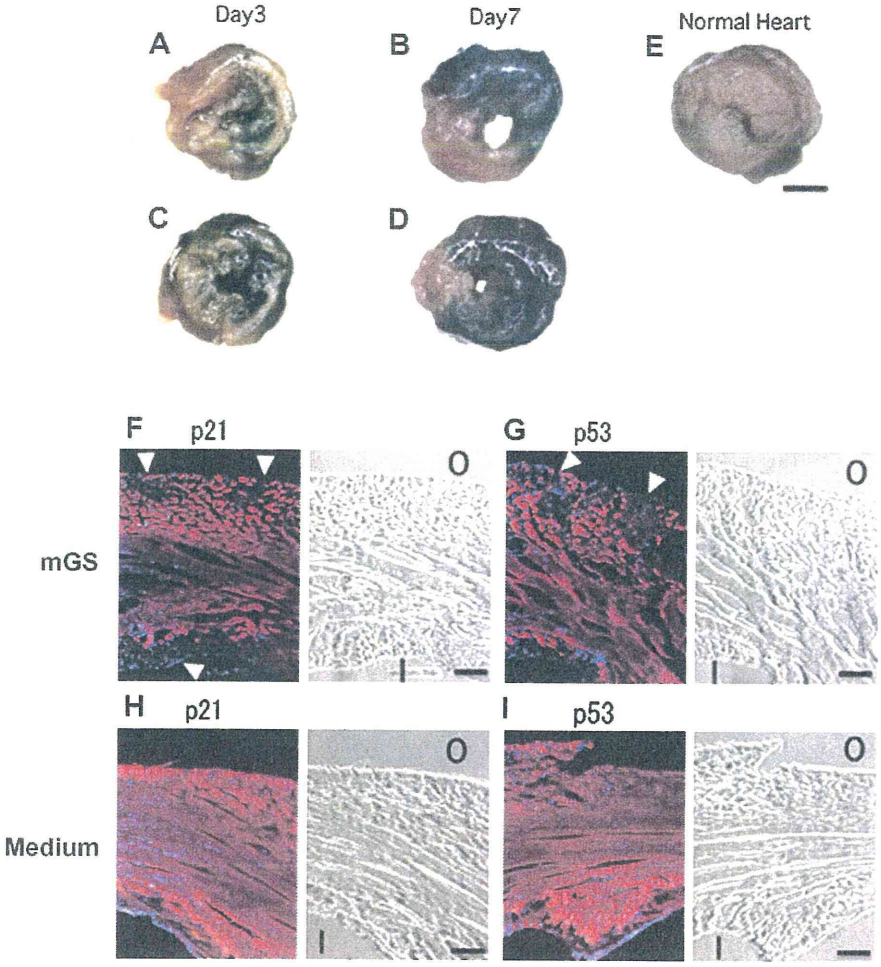

Fig. 4. (A–D) β-Galactosidase staining was detected 3 days (A) and 7 days (B) after Flk1$^+$ mGS cell transplantation. β-Galactosidase staining was also detected 3 days (C) and 7 days (D) after control medium injection. (E) β-Galactosidase staining was not detected in the non-ischemic normal heart. Scale bar: 1 mm. (F,G) Activated p21 and p53 were not clearly detected in the epicardium and endocardium of infarcted areas in Flk1$^+$ mGS cell-transplanted hearts (arrowheads). (H,I) Activated p21 and p53 were clearly detected in the epicardium and endocardium of the infarcted area in medium injected hearts. The nuclei were counterstained with Hoechst 33342 (blue). Bar; 50 μm. O, Outside the left ventricle. I, Inside the left ventricles. (For interpretation of the references to colour in this figure legend, the reader is referred to the web version of this article.)

ate into cardiomyocytes and endothelial cells *in vitro* and *vivo* [22], indeed, but judging from *in vitro* differentiation capacity, mGS cells, which have equal potential in differentiation into endothelial cells to ES cells, have much priority.

Furthermore, the use of mGS cells in cardiac regeneration therapy for ischemic heart disease has much advantage. In the pluripotent or multipotent stem cells, ES cells have ethical problem, adult stem cells have less differentiate potential into cardiomyocyte and endothelial cells than ES cells or mGS cells *in vitro*, and induced pluripotent stem (iPS) cells are consist of transgenes and have a problem to be oncogenic.

Transplantation of the Flk1$^+$ mGS cells improved the left ventricular systolic function and a part of Flk1$^+$ mGS cells could differentiate into cardiomyocytes and endothelial cells *in vivo*. But we could not be sure that only a few numbers of these differentiated cells were sufficient to bear the results of this cardiac functional improvement. However; if we can improve the method of transplantation, it is surely expected that the differentiation potential of Flk1$^+$ mGS into cardiomyocytes and endothelial cells can be remarkably increased *in vivo* compared to other tissue stem cells. In contrast, the Flk1$^-$ mGS cell transplantation did not improve the cardiac function of AMI model mice. And more, we could not detect any differentiated cardiomyocyte or endothelial cell derived from Flk1$^-$ mGS cells in the infarcted area.

Except for the cardiac and endothelial cells differentiation from the transplanted cells, the mechanisms of cardiac function improvement after the cell transplantation were reported previously. Some reported the mechanism was vasculogenesis [2,6,23], and others reported it was anti-apoptotic effect [2] after the cell transplantation for AMI models. In our experiments, the thickness of the infarcted area was significantly larger in the Flk1$^+$ mGS cell transplanted group than in the medium injected group. Simultaneously, angiogenesis in the marginal zone was more frequently detected in the Flk1$^+$ mGS cell transplanted group than that in the medium injected group. Most of these new vessels were not the result of regeneration from the transplanted Flk1$^+$ mGS cells, but the result of the angiogenesis from the host cells. These results indicate that the sufficient blood perfusion resulting from enough angiogenesis enables host cardiomyocytes to survive after Flk1$^+$ mGS cells transplantation. At this time, we questioned why angiogenesis is enhanced specifically after the Flk1$^+$ mGS cells transplantation and not after the medium injection. Furthermore, we investigated the cell death mechanism after cell transplantation. We first investigated the anti-apoptotic effect of cell transplantation. But the

anti-apoptotic effect was not clearly revealed by the TUNEL staining in our experiments. Gonzalez et al. previously reported that activation of cardiac progenitor cells reversed senescence and improved the cardiac function in the failing heart [16]. Because we think that the Flk1$^+$ mGS cells are similar to cardiac stem/progenitors cells, a similar phenomenon may occur after the Flk1$^+$ mGS cell transplantation. The reduction effect of senescence may occur in the transplantation of ES cells, adipose tissue stem cells or bone marrow derived cells, further examination is needed for selecting the most effective cells from these cell source and mGS cells. In the β-galactosidase assay, cell death via senescence was clearly inhibited at the early phase of AMI after the Flk1$^+$ mGS cells transplantation. In addition, the signals p21 and p53 were activated in senescent cells and both signals were especially inhibited around the epicardial layers in the infarcted area at the very early phase of AMI. From these results, Flk1$^+$ mGS cell transplantation first prevents cell senescence in infarcted areas at the very early phase of ischemia. Next, angiogenesis from transplanted cells was enhanced during this period. Finally, a number of original host cardiomyocytes survived in the Flk1$^+$ mGS cell transplanted group. We think that the cardiac function of the Flk1$^+$ mGS cell transplanted group was significantly improved through these hypothetical mechanisms. Above these insights, we expect both the effect of angiogenesis and the reduction effect of senescence simultaneously from Flk1$^+$ mGS transplantation *in vivo* when we can improve the method of the cell transplantation to ischemic heart.

In conclusion, the transplanted Flk1$^+$ mGS cells improved the cardiac function in the AMI model mice and we observed that these cells differentiate into cardiomyocytes and endothelial cells. In addition, they prevented host cardiomyocytes death mainly through inhibition of senescence. Of course, these mechanisms require further investigation. When these mechanisms become more clearly elucidated, we hope that in the pluripotent or multipotent stem cells which are available for clinical application of cardiac regeneration therapy, Flk1$^+$ mGS cell transplantation will have advantage in the therapy for AMI patients.

Conflict of Interest

None.

Acknowledgments

We thank Dr. Kodama for kindly providing the OP-9 stromal cell line. This study was supported by the Program for Promotion of Fundamental Studies in Health Science of the National Institute of Biomedical Innovation (NIBIO) (03-2) and Research of Japan and by a Grant-in-Aid for Creative Scientific Research (13GS0009).

References

[1] S.W. Etoch, S.C. Koenig, M.A. Laureano, et al., Results after partial left ventriculectomy versus heart transplantation for idiopathic cardiomyopathy, J. Thorac. Cardiovasc. Surg. 117 (5) (1999) 952–959.
[2] A.A. Kocher, M.D. Schuster, M.J. Szabolcs, et al., Neovascularization of ischemic myocardium by human bone-marrow-derived angioblasts prevents cardiomyocyte apoptosis, reduces remodeling and improves cardiac function, Nat. Med. 7 (4) (2001) 430–436.
[3] A.P. Beltrami, L. Barlucchi, D. Torella, et al., Adult cardiac stem cells are multipotent and support myocardial regeneration, Cell 114 (6) (2003) 763–776.
[4] F.D. Pagani, H. DerSimonian, A. Zawadzka, et al., Autologous skeletal myoblasts transplanted to ischemia-damaged myocardium in humans. Histological analysis of cell survival and differentiation, J. Am. Coll. Cardiol. 41 (5) (2003) 879–888.
[5] S. Baba, T. Heike, M. Yoshimoto, et al., Flk1(+) cardiac stem/progenitor cells derived from embryonic stem cells improve cardiac function in a dilated cardiomyopathy mouse model, Cardiovasc. Res. 76 (1) (2007) 119–131.
[6] A.A. Kocher, M.D. Schuster, N. Bonaros, et al., Myocardial homing and neovascularization by human bone marrow angioblasts is regulated by IL-8/Gro CXC chemokines, J. Mol. Cell. Cardiol. 40 (4) (2006) 455–464.
[7] S.I. Nishikawa, S. Nishikawa, S. Hirashima, et al., Progressive lineage analysis by cell sorting and culture identifies FLK1+VE-cadherin+ cells at a diverging point of endothelial and hemopoietic lineages, Development 125 (9) (1998) 1747–1757.
[8] M. Iida, T. Heike, M. Yoshimoto, et al., Identification of cardiac stem cells with FLK1, CD31, and VE-cadherin expression during embryonic stem cell differentiation, FASEB J. 19 (3) (2005) 371–378.
[9] M. Kanatsu-Shinohara, K. Inoue, et al., Generation of pluripotent stem cells from neonatal mouse testis, Cell 119 (7) (2004) 1001–1012.
[10] S. Baba, T. Heike, K. Umeda, et al., Generation of cardiac and endothelial cells from neonatal mouse testis-derived multipotent germline stem cells, Stem Cells 25 (6) (2007) 1375–1383.
[11] M. Hirashima, H. Kataoka, S. Nishikawa, et al., Maturation of embryonic stem cells into endothelial cells in an *in vitro* model of vasculogenesis, Blood 93 (4) (1999) 1253–1263.
[12] M. Ogawa, M. Kizumoto, S. Nishikawa, et al., Expression of alpha4-integrin defines the earliest precursor of hematopoietic cell lineage diverged from endothelial cells, Blood 93 (4) (1999) 1168–1177.
[13] T. Minamino, T. Yoshida, K. Tateno, et al., Ras induces vascular smooth muscle cell senescence and inflammation in human atherosclerosis, Circulation 108 (18) (2003) 2264–2269.
[14] T. Minamino, H. Miyauchi, T. Yoshida, I. Komuro, Endothelial cell senescence in human atherosclerosis: role of telomeres in endothelial dysfunction, J. Cardiol. 41 (1) (2003) 39–40.
[15] C. Chimenti, J. Kajstura, D. Torella, et al., Senescence and death of primitive cells and myocytes lead to premature cardiac aging and heart failure, Circ. Res. 93 (7) (2003) 604–613.
[16] A. Gonzalez, M. Rota, D. Nurzynska, et al., Activation of cardiac progenitor cells reverses the failing heart senescent phenotype and prolongs lifespan, Circ. Res. 102 (5) (2008) 597–606.
[17] B.D. Chang, Y. Xuan, E.V. Broude, et al., Role of p53 and p21waf1/cip1 in senescence-like terminal proliferation arrest induced in human tumor cells by chemotherapeutic drugs, Oncogene 18 (34) (1999) 4808–4818.
[18] X. Zhang, J. Li, D.P. Sejas, Q. Pang, The ATM/p53/p21 pathway influences cell fate decision between apoptosis and senescence in reoxygenated hematopoietic progenitor cells, J. Biol. Chem. 280 (20) (2005) 19635–19640.
[19] G.V. Silva, E.C. Perin, H.F. Dohmann, et al., Catheter-based transendocardial delivery of autologous bone-marrow-derived mononuclear cells in patients listed for heart transplantation, Tex. Heart Inst. J. 31 (3) (2004) 214–219.
[20] N. Hattan, H. Kawaguchi, K. Ando, et al., Purified cardiomyocytes from bone marrow mesenchymal stem cells produce stable intracardiac grafts in mice, Cardiovasc. Res. 65 (2) (2005) 334–344.
[21] M.A. Laflamme, K.Y. Chen, A.V. Naumova, et al., Cardiomyocytes derived from human embryonic stem cells in pro-survival factors enhance function of infarcted rat hearts, Nat. Biotechnol. 25 (9) (2007) 1015–1024.
[22] Y. Yamada, S. Yokoyama, X. Wang, et al., Cardiac stem cells in brown adipose tissue express CD133 and induce bone marrow nonhematopoietic cells to differentiate into cardiomyocytes, Stem Cells 25 (2007) 1326–1333.
[23] M.D. Schuster, A.A. Kocher, T. Seki, et al., Myocardial neovascularization by bone marrow angioblasts results in cardiomyocyte regeneration, Am. J. Physiol. Heart Circ. Physiol. 287 (2) (2004) H525–H532.

Transmission distortion by loss of p21 or p27 cyclin-dependent kinase inhibitors following competitive spermatogonial transplantation

Mito Kanatsu-Shinohara[a,1], Seiji Takashima[a], and Takashi Shinohara[a,b]

[a]Department of Molecular Genetics, Graduate School of Medicine, Kyoto University, Kyoto 606-8501 Japan; and [b]Japan Science and Technology Agency, Japan Science and Technology Agency, Kyoto 606-8501 Japan

Edited by Ryuzo Yanagimachi, The Institute for Biogenesis Research, University of Hawaii, Honolulu, HI, and approved March 1, 2010 (received for review December 16, 2009)

Spermatogonial stem cells (SSCs) undergo self-renewal division to support spermatogenesis. Although several positive regulators of SSC self-renewal have been identified, little is known about the mechanisms that negatively regulate SSCs. Here we developed a novel transplantation assay for SSCs and demonstrate that p21 and p27 cyclin-dependent kinase inhibitors play critical roles in SSC self-renewal and differentiation. Overexpression of p21 or p27 abrogated proliferation of cultured SSCs in vitro, and their expression levels were downregulated by exogenous self-renewal signals. In contrast, no apparent defects were found in p21 or p27-deficient SSCs by spermatogonial transplantation. However, competitive spermatogonial transplantation with WT SSCs revealed that the loss of either gene causes distortion of germline transmission: p21-deficiency facilitated mutant offspring production, whereas germline transmission was limited by p27-deficiency. Serial transplantation also showed that the loss of p27, but not p21, decreases secondary colony formation, suggesting that appropriate amounts of p27 are necessary for sustaining SSC self-renewal. Thus, p21 and p27 cyclin-dependent kinase inhibitors play critical roles in germline transmission by regulating the balance between SSC self-renewal and differentiation, and competitive spermatogonial transplantation technique will be useful for analyzing subtle defects in spermatogenesis that are not evident by traditional spermatogonial transplantation.

germline transmission | spermatogenesis | stem cell | cyclin-dependent kinase inhibitor | self-renewal

Spermatogenesis is a dynamic and complex process based on the self-renewal division of spermatogonial stem cells (SSCs). Very few SSCs are found in the testis (0.02–0.03% in a testis cell suspension), but SSCs proliferate throughout life to support spermatogenesis (1, 2). The balance between SSC self-renewal and pool size necessitates strict control, because excessive self-renewal or differentiation can cause male infertility. Although stem cells are relatively cytokine resistant in many tissues, glial cell line-derived neurotrophic factor (GDNF) promotes self-renewal division of SSCs (3). Changes in GDNF levels greatly impact on spermatogenesis in vivo: Excessive GDNF expression induces the accumulation of undifferentiated spermatogonia, whereas decreases in GDNF cause hypospermatogenesis and the gradual loss of SSCs (3). Thus, the regulation of SSC self-renewal is governed by a subtle balance between negative regulatory pathways that maintain mitotic quiescence and positive growth-promoting signals involving GDNF. Although we recently discovered that the Ras-cyclin D2 pathway acts downstream of GDNF to promote SSC self-renewal (4), little is known about how the balance between self-renewal and differentiation is maintained in vivo.

Cyclin-dependent kinase inhibitors (CDKIs) are good candidates for the negative regulation of SSC proliferation. Two families of CDKIs promote cell cycle withdrawal by blocking the activity of cyclin/CDK complexes: the Cip/Kip family, including p21, p27, and p57, and the INK4 family, including p15, p16, p18, and p19 (5). Whereas INK4 proteins bind to CDK4 or CDK6 and inhibit their activity, Cip/Kip proteins show a broader range of activities and interact with all cyclin/CDK complexes. Cip/Kip proteins are distinct from the INK4 family in that they also stimulate the formation of cyclin D/CDK4/6 complexes to promote proliferation (6). Importantly, Cip/Kip proteins have additional functions beyond regulating cell divisions and regulate differentiation. For example, enforced expression of p21 or p27 induces the differentiation of neuroblastoma cells and myelomonocytic leukemia cells (6). Although KO mice have been produced for Cip/Kip family genes, no apparent SSC phenotype has been reported, and the effects of these genes remain unclear (7, 8).

Because stem cells comprise only a small population and are defined retrospectively through the analysis of daughter cells, studies to analyze SSCs have been hampered by difficulties in distinguishing SSCs from committed spermatogonia. In 1994, however, a spermatogonial transplantation technique was developed (9). With this technique, SSCs can be detected by their ability to generate germ cell colonies after microinjection into seminiferous tubules of infertile recipient animals. Eventually, recipient animals can produce donor-derived offspring by mating with WT females. Because differentiated progenitor cells do not have self-renewal capacity, only SSCs can produce these results. Although this technique has been used extensively to study SSCs, the degree of SSC self-renewal and differentiation is difficult to evaluate by morphological analyses of germ cell colonies. Moreover, measurements of SSC numbers do not necessarily correlate with long-term functional capacities. In fact, declining fertility is reported after serial SSC transplantation, which raised question about whether transplanted SSCs are fully competitive as WT SSCs before transplantation (10).

In the present study, we report a unique SSC transplantation assay, in which stem cell function of a mutant donor is assayed by mixing with WT SSCs. Although spermatogonial transplantation failed to reveal abnormalities in p21 and p27 KO SSCs, p21 and p27 deficiencies have contrasting effects on germline transmission efficiency when they were mixed with WT SSCs. Moreover, serial transplantation showed decreased secondary colony production from p27 KO SSCs. This strategy of SSC analysis will be useful for comparing long-term SSC function and is capable of detecting subtle defects that escape detection by conventional transplantation technique.

Author contributions: M.K.-S. and T.S. designed research; M.K.-S., S.T., and T.S. performed research; M.K.-S. and T.S. analyzed data; and M.K.-S. and T.S. wrote the paper.

The authors declare no conflict of interest.

This article is a PNAS Direct Submission.

[1]To whom correspondence should be addressed. E-mail: mshinoha@virus.kyoto-u.ac.jp.

This article contains supporting information online at www.pnas.org/cgi/content/full/0914448107/DCSupplemental.

Results

Effects of p21 and p27 CDKIs on Cultured SSCs. To identify molecules that negatively regulate SSC proliferation, we used germline stem (GS) cells, cultured SSCs (11). The addition of GDNF and EGF and/or basic fibroblast growth factor (bFGF) induces SSC proliferation in vitro. Approximately 1–2% of the GS cells have SSC activity (4). GS cells from WT mice were infected with lentivirus vectors expressing candidate genes and Venus fluorescent marker gene under the control of an elongation factor2 promoter. Using this strategy, we found that overepression of p21 or p27 CDKIs compromises GS cell proliferation. When the transfected cells were analyzed 3 d after infection, significantly smaller numbers of Venus$^+$ cells were found after CDKI overexpression in all six separate experiments (Fig. S1 *A* and *B*). In particular, very few germ cell clumps showed fluorescence after p21 overexpression, suggesting that the transfected cells proliferated more slowly than WT cells or died shortly after transfection. Some clumps, however, remained after p27 overexpression at 21 d, but significantly fewer clumps were observed as compared to controls (Fig. S1*C*). In contrast, cells transduced with an empty vector showed strong fluorescence and the cells could be passaged every 5–6 d. Flow cytometric analysis at 10 d postinfection also confirmed the reduction in Venus$^+$ cells after CDKI overexpression. Cell cycle analyses also showed the growth suppression due to p21 overexpression (Fig. S1*D*).

We then examined whether p21 or p27 expression is influenced by exogenous cytokines. Real-time PCR analysis showed a significant reduction in p21 and p27 expression due to cytokine stimulation (Fig. S1*E*). The combination of EGF and bFGF showed a comparable effect as GDNF, and the addition of all cytokines suppressed the p21 and p27 levels to 25.8% and 19.0%, respectively. These in vitro results indicated that p21 and p27 CDKI levels are regulated by exogenous cytokines and also suggested that both genes may negatively regulate SSC proliferation in vivo.

SSC Activity of p21 and p27 KO Testis Cells After Spermatogonial Transplantation. To examine the effects of p21 and p27 genes in vivo, we analyzed testes of p21 and p27 KO mice. Both mutant mice survived to birth and matured into adults. Whereas p21 KO mice appeared normal, p27 KO mice exhibited multiple organ hyperplasia and females were infertile due to poor ovarian follicle development (7, 8). In contrast, both p21 and p27 KO males produced spermatozoa and were fertile, suggesting normal spermatogenesis. However, whereas testes from p21 KO mice were comparable to those of WT mice, testes from p27 KO mice were significantly larger (Fig. 1*A*). Although flow cytometry showed normal size of p21 and p27 KO spermatogonia, cell cycle analyses revealed that EpCAM$^+$ spermatogonia from both mutants proliferated more actively than those of WT mice, and significantly more cells were found in the G2/M phase (Fig. 1*B*). However, whereas real-time PCR analyses showed no compensatory upregulation of p21 or p27 in either type of KO mice, expression of E-cadherin or promyelocytic leukemia zinc finger (PLZF), markers for undifferentiated spermatogonia (12–14), was significantly reduced (Fig. 1*C*), suggesting that undifferentiated spermatogonia in these mice comprise relatively smaller population.

To study the function of SSCs, we used spermatogonial transplantation (Fig. 1*D*). Donor testis cells were marked by mating the KO animals with a transgenic mouse line C57BL6/Tg14 (act-EGFP-OsbY01) (green mice) that ubiquitously expresses enhanced green fluorescent protein (EGFP). Preliminary transplantation of mutant cells into nonablated WT testis did not result in colonization, thus suggesting that mutant SSCs do not have an enhanced ability to compete for the niche that is occupied by WT SSCs. We then transplanted the mutant cells into empty tubules to quantify SSC number. In three separate experiments, the same number of mutant and WT testis cells were transplanted into adult WBB6F1-W/W^v(W) mice that were deficient for spermatogenesis due to c-kit gene defects (15). Two months after transplantation, the recipient mice were sacrificed and their testes were analyzed for colonization under UV light.

Both p21 and p27 KO donor cells produced germ cell colonies that were similar to those of WT mice. We found no apparent abnormalities in the length and the morphology of the colonies, which suggested normal proliferation and differentiation of transplanted SSCs (Fig. 1*D*). The p21 KO cells and WT cells produced 4.7 ± 0.8 and 4.2 ± 0.5 colonies of donor-derived spermatogenesis/10^5 cells injected, respectively, and this difference was not statistically significant (Fig. 1*E*). In contrast, the p27 KO cells produced significantly smaller numbers of colonies as compared to WT cells, and the number of colonies generated was 2.0 ± 0.5 and $3.8 \pm 0.5/10^5$ cells injected for p27 KO cells and WT cells, respectively. Because each colony was derived from a single transplanted SSC (16, 17), these results indicated that the SSC concentration in p27 KO mice was significantly lower than that of WT mice. Although the total number of SSCs per testis (cell recovery × concentration of SSCs in the injected cell suspension determined by transplantation) was increased for the WT background (1482 vs. 1160 for WT and p27 KO cells), the difference was not significant. These results show that both p21 and p27 KO testis contain similar numbers of SSCs.

Transmission Distortion by Competitive Spermatogonial Transplantation. Although these transplantation experiments showed no apparent SSC abnormalities, we speculated that subtle imbalances in SSC self-renewal and differentiation might not be evident in a morphological analysis of germ cell colonies using a simple transplantation assay. To overcome this problem, we cotransplanted WT and mutant cells into the same recipient, and analyzed cell differentiation potential by confirming the genotype of the offspring (Fig. 2*A*). We collected single cell suspensions from p21 or p27 KO pup testes that were enriched for SSCs due to the absence of differentiated cells (18). Testis cells from each mutant mouse were mixed at a 1:1 ratio with those from control WT mice of the same age. The mixed testis cells were then transplanted into 5–10 day old W recipient pups to produce offspring from the transplanted SSCs. Previously, we showed that immature recipients are superior to adult recipients in restoring fertility due to the enhanced SSC colonization (18). Recipient males were housed with two or three WT B6 females, at least 4 weeks after transplantation. Two separate experiments were performed for p21 KO mice, whereas three experiments were carried out for p27 KO mice. About 3×10^5 cells were transplanted into each recipient testis.

Within 3 months after transplantation, 3/8 and 3/9 recipient males that received p21 or p27 KO SSCs, respectively, became fertile (Table S1). Histological analyses of both types of recipients confirmed normal spermatogenesis (Fig. 2*B*). When the offspring genotypes were confirmed by genomic PCR using tail DNA, transmission rate distortion of the donor haplotype was noted in both experiments (Fig. 2 *C* and *D*). For p21 experiments, 212 offspring were produced from the three recipients, and the animals were maintained as long as 304 d after transplantation. PCR analysis revealed that 206/212 offspring contained the neo gene. All of these offspring were heterozygous for the p21 gene, because the recipient males were mated with WT females. The percentage of these heterozygous males was $97.2 \pm 1.8\%$ from each recipient. In contrast, for p27 experiments, a total of 98 offspring were produced during 205 d from the three recipients that received p27 KO testis cell transplantation. WT offspring, however, were predominantly produced from the recipients, and only 12/98 offspring were heterozygous for the p27 gene. Although the overall percentage of heterozygous offspring was 12.2%, one of the recipient males produced as many as 10 heterozygous offspring. Moreover, these offspring were born

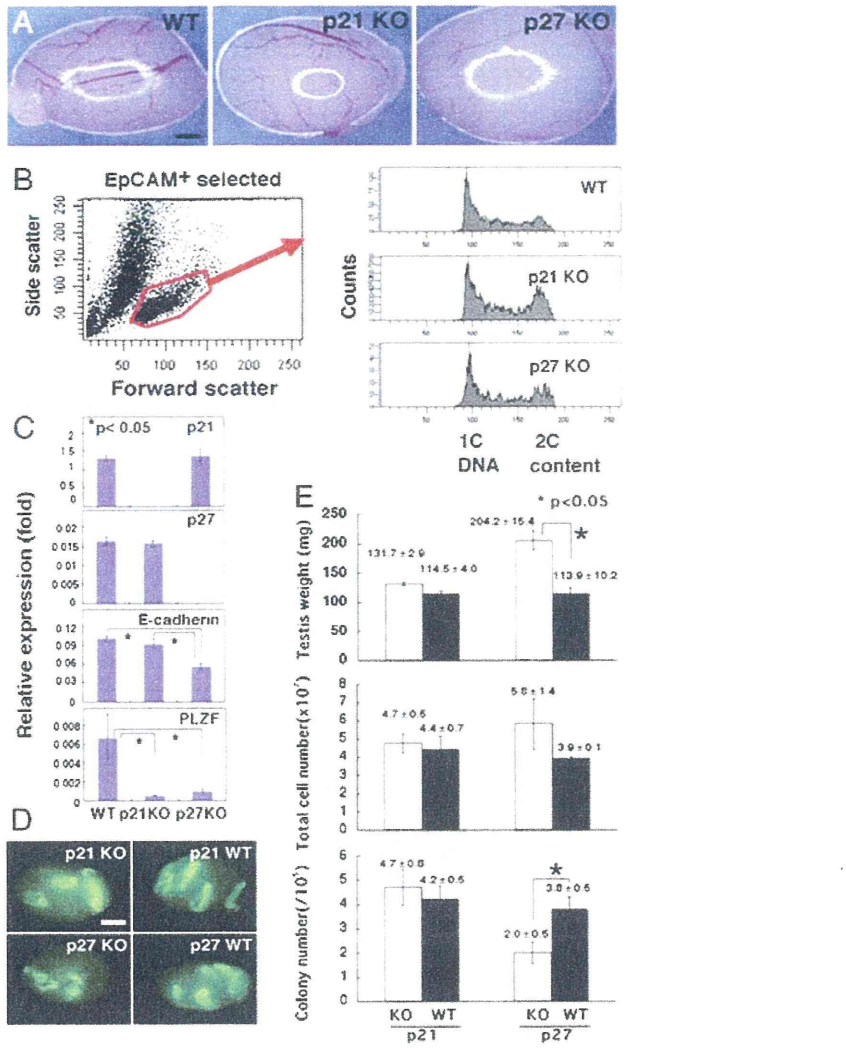

Fig. 1. Phenotypic and functional analyses of p21 or p27 KO testis cells. (*A*) Appearance of mutant testes. Note the larger size of the p27 KO testis. (*B*) Cell cycle analysis of EpCAM$^+$ spermatogonia. Note the enhanced proliferation of p21 and p27 KO cells. WT mice were used as a control. (*C*) Real-time PCR analyses of p21, p27, E-cadherin, and PLZF expression. Expression of E-cadherin or PLZF was significantly downregulated in the mutant mice. (*D*) Macroscopic appearance of the recipient testes. Green fluorescence indicates donor cell colonization. (*E*) Testis weight (*Upper*, $n = 3$), total cell number after enzymatic digestion (*Middle*, $n = 3$), and colony number (*Lower*, $n = 15$–17). Asterisks denote significant differences compared to the control ($P < 0.01$). Bar = 1 mm (*A* and *D*).

within 98 d after transplantation, and no heterozygous offspring were produced from this male up to 195 d.

Impact of p21 and p27 Deficiencies in Self-Renewal Divisions of SSCs. To directly examine the impact of p21- and p27-deficiency on SSC self-renewal, we performed serial transplantation (Fig. 3*A*). In normal testes, SSCs are kept under constant pressure to differentiate and produce sperm. The most generally accepted hypothesis is that SSCs undergo only two types of cell division: They produce either two stem cells (self-renewal division) or two progenitor cells (differentiating division) (1). Each division occurs at about the same frequency. After transplantation, however, SSCs are thought to undergo self-renewal divisions more frequently than differentiation divisions, and thus increase their numbers (19). Because the number of colonies in the recipient testis indicates the number of SSCs that initially colonized the testis, the number of SSCs that were produced by subsequent divisions may be determined by transplantation into another testis. We collected testis cells from WT and mutant donors that contained the EGFP transgene. After dissecting out colonies in each recipient testis at 10 weeks posttransplantation, the tubules were dissociated into single cells and suspended in 15–21 μl of injection medium. The number of cells recovered from the three types of recipients ranged from $0.4 - 3.0 \times 10^6$ cells, with an average of 1.6×10^6 cells. Differences among donors were not significant. Approximately 4 μl of the cell suspension was microinjected into three secondary recipient testes.

Analysis of the secondary recipient testes at 2 months after transplantation revealed that significantly fewer SSCs were produced from the p27 KO donor testis cells (Fig. 3 *B* and *C*). Although 13/14 transplantations showed colony number increases (total regenerated colony number—primary colony number used for transplantation) in experiments using WT and p21 KO mice, only 5/14 transplantations showed increase in experiments using p27 KO mice, indicating that the SSCs in p27 KO mice produced smaller numbers of secondary colonies. Assuming that 10% of the SSCs can colonize (19), and that each colony is produced by one SSC (16, 17), the multiplication of colony numbers (total regenerated colony number $\times$ 10/primary colony number used for serial transplantation) were

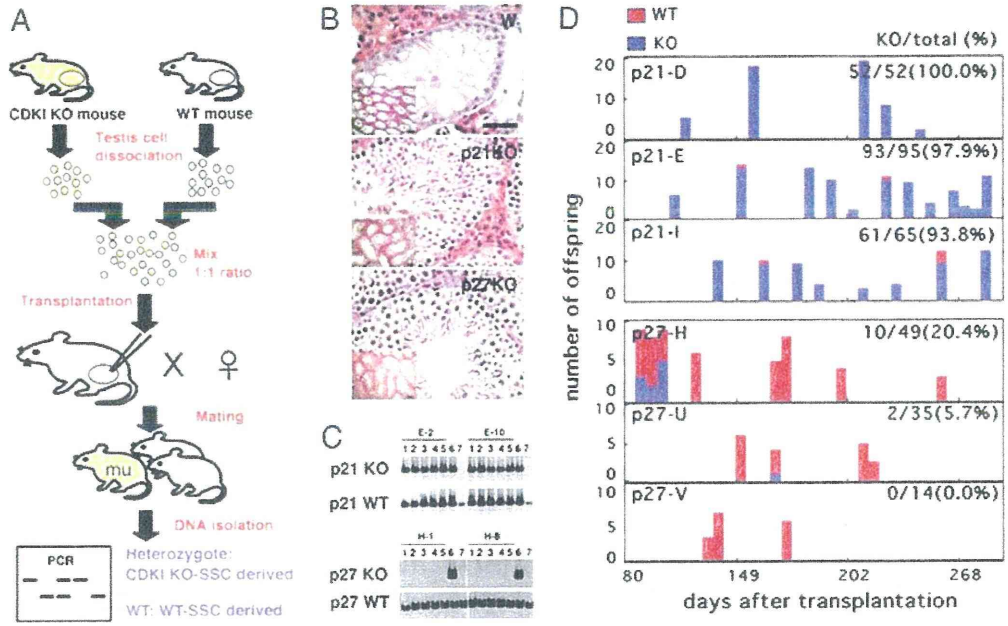

Fig. 2. Competitive spermatogonial transplantation. (*A*) Experimental procedure. Two populations of testis cells, one from a WT mouse and the other from a KO mouse, were mixed at a 1:1 ratio and transplanted into W mice to produce offspring. Tail DNA of the F1 offspring were analyzed by PCR for genotyping. (*B*) Normal appearing spermatogenesis in the recipient testes. (*C*) Genotyping by PCR. (*Upper*) Offspring from recipient E, which were transplanted with a mixture of p21 KO and WT testis cells. Analyses of the second and tenth littermates are shown (*Lanes 1–5*). Lane 6: p21 heterozygous; lane 7: WT control tails. All F1-derived offspring showed p21 mutant bands. (*Lower*) Offspring from recipient H, which were transplanted with a mixture of p27 KO and WT testis cells. Analyses of the second and tenth littermates are shown (*Lanes 1–5*). Lane 6: p21 heterozygous ; lane 7: WT control tails. None of the offspring showed p27 mutant bands. (*D*) Temporal analysis of offspring. Bar = 50 μm, (*B*); 100 μm (*B*, *Inset*).

7.2 ± 1.6 ($n = 14$) and 29.3 ± 4.0 ($n = 14$) for p27 KO cells and WT cells, respectively (Table S2). The difference between p27 KO and WT cells was significant. In contrast, p21 KO cells produced comparable numbers of secondary colonies with WT cells, and the average number of colonies per primary colony was 26.6 ± 5.9 ($n = 14$). No significant difference was observed in the self-

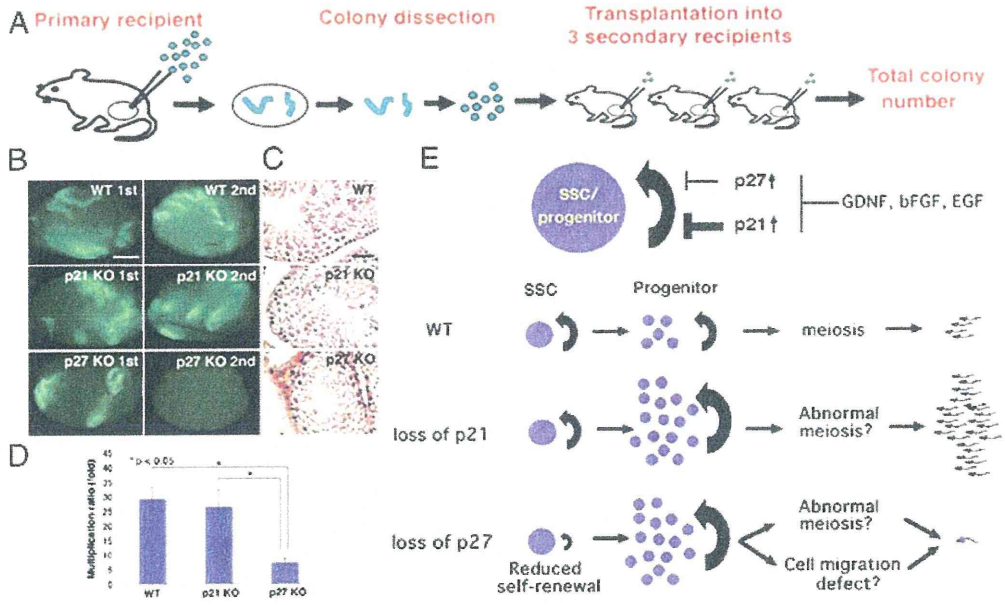

Fig. 3. Serial transplantation. (*A*) Experimental procedure. Colonies in the primary recipients were dissected out at 10 weeks after transplantation, and a portion of them was transplanted into the three testes of the secondary recipients. (*B*, *C*) Macroscopic (*B*) and histological (*C*) appearance of the recipient testes. Green fluorescence indicates donor cell colonization. Note the decrease in secondary colony numbers from p27 KO testis cells. (*D*) The degree of secondary colony formation, indicated by the ratio of SSC number between the two time points. Asterisks denote significant differences compared to the control ($P < 0.01$). (*E*) Summary of results and models for transmission distortion of p21 and p27 SSCs. (*Upper*) Upregulated p21 or p27 inhibits SSC/progenitor cell proliferation. Exogenous cytokines downregulate p21 and p27 expression. (*Lower*) Loss of p21 does not influence SSC self-renewal, but likely enhances progenitor cell proliferation. In contrast, loss of p27 decreased SSC self-renewal but may enhance progenitor cell proliferation. However, these progenitor cells have defects in meiosis and/or cell migration, both of which may have caused decreased spermatogenesis efficiency. Bar = 1 mm (*B*); 100 μm (*C*).

renewal capacity of SSCs between p21 KO and WT cells. The doubling times of the SSCs during the 10-week period were 14.4, 14.8, and 24.6 d for WT, p21 KO, and p27 KO SSCs, respectively (Fig. 3*D*).

Discussion

Spermatogonial transplantation technique provided the first functional assay for SSCs. It has been used to detect SSCs and determine whether abnormal spermatogenesis is caused by germ cell defects or their respective microenvironments. This technique is also useful for assessing SSC numbers quantitatively. For example, when a mixture of two testis cell populations were transplanted at a 1:1 ratio, recipient testes contained a near 1:1 ratio of colonies with each of the two genotypes (16). However, spermatogenesis is not completely normal after transplantation, and multiple abnormalities that are associated with transplantation, such as increased apoptosis or missing layers of germ cells (20), raise questions about the efficiency and quality of spermatogenesis after transplantation. In this study, we developed a competitive spermatogonial transplantation technique to provide a selective pressure to identify SSCs with high capacity for competitive long-term repopulation. In its concept and design, the technique is somewhat similar to competitive repopulation technique in hematopoietic stem cells (HSCs) (21). Forced competition against WT SSCs allowed direct functional comparisons between the two donors in a quantitative manner under consistent microenvironmental stimuli. Using this method, growth factors, nutrient conditions, and systemic environments such as hormonal levels are provided equally for both donors in the same recipient animal. This was particularly important in this study, because abnormalities are reported for both Sertoli and Leydig cells in p27 KO mice (22, 23). Furthermore, although periodic sperm sampling from the same individual is difficult in mice, this technique allows for the monitoring donor cell dynamics over a long period. Thus, competitive spermatogonial transplantation will be useful for functional analyses of spermatogenesis.

Using this technique, we found transmission distortion of mutant SSCs with contrasting results: p21-deficiency facilitated the production of mutant offspring, whereas it was severely limited by p27-deficiency. In contrast, p21 and p27 overexpression inhibited GS cell proliferation. These results suggested that p21 and p27 levels are important in maintaining normal proliferation of SSCs and/or progenitor cells. In fact, studies of other self-renewing tissues also suggested the involvement of CDKIs in regulating the stem cell quiescence and pool size. In general, p21 is thought to act on quiescent stem cells, whereas p27 is a progenitor-specific inhibitor for repopulation efficiency (24). During hematopoiesis, for example, whereas p21 governs cell cycle entry of HSCs, p27 does not affect HSC number, cell cycling, or self-renewal but has an impact on the cell cycle of progenitors (24). Likewise, p21-deficiency influences the number and proliferation of neural stem cells (NSCs) (25). Although mutant animals initially have increased numbers of NSCs due to excessive proliferation, the levels decrease as they age due to exhaustion.

Recent studies using male germ cells also suggest that p21 plays an important role in SSCs: Atm-deficient undifferentiated spermatogonia upregulates p21, which is responsible for cell cycle arrest upon DNA damage (26). Suppression of p21 can partially restore SSC activity in Atm KO mice, but its normal function remains unclear. In this study, we showed that p21 levels are regulated by exogenous cytokines and that ectopic overexpression of p21 leads to growth inhibition. In contrast, p21-deficiency does not alter SSC number or self-renewal activities, which suggested that transmission distortion was caused by defects in more differentiated cells. On the other hand, reduced PLZF expression suggested smaller size of undifferentiated spermatogonia population, and these conflicting observations make it difficult to explain why germline transmission occurred predominantly from p21 KO cells. Nevertheless, given the increased mitotic activity of whole spermatogonia population, we speculate that more differentiated type of spermatogonia, such as type A_{1-4} or B spermatogonia, are proliferating more actively and caused transmission distortion by increasing the population size or differentiating faster. Alternatively, it may result from an advantage of p21 KO germ cells to progress through meiosis; p21 is most strongly expressed in pachytene spermatocytes and spermatids in normal testis.

On the other hand, p27-deficiency had a direct effect on SSC. We initially assumed that p27-deficiency would not influence germline transmission, because Sertoli cells have been hypothesized as being responsible for the large testis phenotype of p27 KO mice: p27 has been detected only in Sertoli cells and germ cells were thought to be normal (27). However, offspring were rarely produced from p27 KO cells after competitive transplantation, which suggested defects in germ cells. Although the possibility of Sertoli cell colonization cannot be totally excluded, another study also showed the important role of p27 in germ cells: mice deficient in Skp2, which mediates ubiquitin-dependent degradation of p27, exhibited a progressive loss in spermatogenic cells (28). Furthermore, disruption of p27 in these mice restored fertility, suggesting that testicular hypoplasia of Skp2 mutant mice is attributable to the antiproliferative effects of p27 accumulation. Therefore, although p27 has not been detected at protein levels in the germline, these results suggest that germ cells also contribute to the large testis phenotype of p27 KO mice, and that it probably has an important influence on the fate decision of SSCs.

Although p27 KO mice show a comparable number of SSCs per testis, our serial transplantation experiments showed reduced secondary colony formation from p27 KO SSCs. It is possible that loss of p27 might have accelerated senescence/differentiation. However, because p27 KO mice remain fertile for long-term and produce significantly more sperm than WT mice (23), we rather speculate that decreases in p27 levels in SSCs may enhance the production of progenitor cells by increasing the relative frequency of differentiating divisions. On the other hand, we also showed using GS cells that p27 overexpression compromises proliferation and that increase in self-renewal factors decreases p27 mRNA levels. Besides transcriptional regulation, p27 is also regulated by protein degradation (29). We recently found that self-renewal signals promote the export of p27 from the GS cell nucleus (4). Therefore, appropriate levels of p27, as well as its cellular location, are required for undergoing self-renewal divisions, and this appears to be regulated in a sophisticated manner by changes in the local self-renewal factor levels in the seminiferous tubules. Disturbance in this regulation may cause abnormalities in SSC self-renewal.

Besides regulating mitosis, p27 is involved in meiosis. Testes from p27 KO mice have a significant number of abnormal leptotene spermatocytes that cannot enter the meiotic prophase (27). Strikingly, some of these spermatocytes attempted to carry out mitotic divisions instead of entering into prophase. Furthermore, p27 KO cells may have impaired migratory activity: p27 binds to RhoA and inhibits its activation by interfering with the interaction between RhoA and its activators (30). Impaired migratory activity can interfere with several steps of spermatogenesis, such as the migration of preleptotene spermatocytes through the blood–testis barrier. Collectively, these factors may have decreased the efficiency of spermatogenesis and caused transmission distortion despite the expanded pool of progenitor cells (Fig. 3*E*).

Our study revealed a critical role for p21 and p27 CDKIs in regulating germline transmission from SSCs. Although the small population size of SSCs makes it difficult to study their dynamics, competitive spermatogonial transplantation techniques have proved to be more sensitive in detecting subtle abnormalities

in spermatogenesis in a quantitative manner. Moreover, serial transplantation techniques were instrumental in analyzing effects on SSC self-renewal. This strategy of analyzing the dynamics of SSCs in vivo can be extended to different mouse mutants, and further analysis of CDKIs will help to determine how self-renewal and differentiation are differentially regulated in SSCs.

Materials and Methods

Animals and Transplantation. The p21 KO mice were purchased from the Jackson laboratory, and p27 KO mice were kindly provided by K. Nakayama (Kyushu University). Both strains of mice were maintained on a B6 background. In some experiments, we also used a Green mouse that expressed the EGFP gene ubiquitously to mark the donor cells (M. Okabe, Osaka University). For spermatogonial transplantation to quantify SSC number, testis cells were collected from 4–6 week old mice. Donor cells were collected by two-step enzymatic digestion using collagenase and trypsin (both from Sigma). Dissociated cells were introduced into the seminiferous tubules of pup (5–10 d old) or adult (4–6 weeks old) W mice (Japan SLC) via an efferent duct. To produce offspring, testis cells were obtained from 5–10 d old mice. The Institutional Animal Care and Use Committee of Kyoto University approved all of the animal experimentation protocols.

Cell Culture and Transfection. GS cells were cultured on mouse embryonic fibroblasts (MEFs) as described previously using StemPro-34 SFM (Invitrogen) (11). For real-time PCR, the cells were cultured on laminin (20 μg/mL; BD Biosciences) to avoid contamination of MEF-derived RNA. For lentivirus transduction, mouse cDNAs encoding p21 or p27 (both from Addgene) were cloned into CSII-EF-IRES-Venus, and virus particles were produced by transient transfection of 293T cells, as described previously (4). All infections were conducted on MEFs by centrifuging at 3000 × *g* for 1 h at 32 °C in the presence of 10 μg/mL polybrene (Sigma). GS cells were infected overnight at a multiplicity of infection of 35 for overnight (4×10^4 cells/cm^2 in 6-well plate).

PCR. Total RNA was isolated using Trizol reagent, and first strand cDNA was synthesized using Superscript™ II (both from Invitrogen). Real-time PCR was performed using the StepOnePlus™ Real-Time PCR system and *Power* SYBR Green PCR Master Mix (Applied Biosystems) with the PCR primers listed in Table S3. All transcript levels were normalized to those of Hprt1. The PCR conditions were 95 °C for 10 min, followed by 40 cycles at 95 °C for 15 s, and 60 °C for 1 min. Experiments were performed on at least two independent samples, and each PCR was run in triplicate. Genotypes of p21 and p27 KO mice were determined using the PCR primers listed in Table S4.

Analysis of the Recipient Testes. In experiments using Green mice, SSC colonization was determined by observation of fluorescence under UV light. Colonies were defined as germ cell clusters longer than 0.1 mm occupying the entire circumference of the tubule. For the morphological examination, testes were processed for paraffin sectioning and counterstained with hematoxylin and eosin.

Cell Cycle Analysis. Testis cells were selected by rat antimouse EpCAM antibody (G8.8; BD Bioscience) using procedures as previously described (26). EpCAM$^-$ cells were then incubated with Hoechst 33342 (Sigma) at 12.5 μg/mL for 45 min at 37 °C and suspended in phosphate-buffered saline/1% fetal calf serum containing 1 μg/mL propidium iodide (PI; Sigma). Cells were analyzed on a FACSAria2 equipped with a 375-nm UV laser (BD Biosciences). Dead cells and nonspermatogonial cells were gated out by high PI staining and forward scatter.

Statistical Analysis. Results are presented as the mean ± SEM. Data were analyzed using a Student's *t* test. Significant differences in the CDKI expression and serial transplantation were determined by a Tukey's honestly significant differences multiple comparisons test.

ACKNOWLEDGMENTS. We thank Ms. Y. Ogata for technical assistance. This research was supported by the Genome Network Project; Japan Science and Technology Agency; Program for Promotion of Basic and Applied Researches for Innovation in Biooriented Industry; the Ministry of Health, Labour, and Welfare; Senri Life Science Foundation; Novartis Foundation (Japan) for the Promotion of Science; Astellas Foundation for Research on Metabolic Disorders; and the Ministry of Education, Culture, Sports, Science, and Technology, Japan.

1. de Rooij DG, Russell LD (2000) All you wanted to know about spermatogonia but were afraid to ask. *J Androl* 21:776–798.
2. Meistrich ML, van Beek MEAB (1993) *Cell and Molecular Biology of the Testis*, eds C Desjardins and LL Ewing (Oxford Univ Press, New York), pp 266–295.
3. Meng X, et al. (2000) Regulation of cell fate decision of undifferentiated spermatogonia by GDNF. *Science* 287:1489–1493.
4. Lee J, et al. (2009) Genetic reconstruction of mouse spermatogonial stem cell self-renewal in vitro by Ras-Cyclin D2 Activation. *Cell Stem Cell* 5:76–86.
5. Sherr CJ, Roberts JM (2004) Living with or without cyclins and cyclin-dependent kinases. *Genes Dev* 18:2699–2711.
6. Weinberg RA (2007) *The Biology of Cancer*, ed RA Weinberg (Garland, New York), pp 255–306.
7. Brugarolas J, et al. (1995) Radiation-induced cell cycle arrest compromised by p21 deficiency. *Nature* 377:552–557.
8. Nakayama K, et al. (1996) Mice lacking p27 (Kip1) display increased body size, multiple organ hyperplasia, retinal dysplasia, and pituitatry tumors. *Cell* 85:707–720.
9. Brinster RL, Zimmermann JW (1994) Spermatogenesis following male germ-cell transplantation. *Proc Natl Acad Sci USA* 91:11298–11302.
10. Ryu BY, Orwig KE, Oatley JM, Avarbock MR, Brinster RL (2006) Effects of aging and niche microenvironment on spermatogonial stem cell self-renewal. *Stem Cells* 24:1505–1511.
11. Kanatsu-Shinohara M, et al. (2003) Long-term proliferation in culture and germline transmission of mouse male germline stem cells. *Biol Reprod* 69:612–616.
12. Tokuda M, Kadonaga Y, Kurahashi H, Marunouchi T (2007) CDH1 is a specific marker for undifferentiated spermatogonia in mouse testes. *Biol Reprod* 76:130–141
13. Costoya JA, et al. (2004) Essentiial role of Plzf in maintenance of spermatogonial stem cells. *Nat Genet* 36:653–659.
14. Buaas FW, et al. (2004) Plzf is required in adult male germ cells for stem cell self-renewal. *Nat Genet* 36:647–652.
15. Geissler EN, Ryan MA, Housman DE (1988) The dominant white spotting (W) locus of the mouse encodes the c-kit proto-oncogene. *Cell* 55:185–192.
16. Zhang X, Ebata KT, Nagano MC (2003) Genetic analysis of the clonal origin of regenerating mouse spermatogenesis following transplantation. *Biol Reprod* 69:1872–1878.
17. Kanatsu-Shinohara M, et al. (2006) Clonal origin of germ cell colonies after spermatogonial transplantation in mice. *Biol Reprod* 75:68–74.
18. Shinohara T, Orwig KE, Avarbock MR, Brinster RL (2001) Remodeling of the postnatal mouse testis is accompanied by dramatic changes in stem cell number and niche accessibility. *Proc Natl Acad Sci USA* 98:6186–6191.
19. Nagano M, Avarbock MR, Brinster RL (1999) Pattern and kinetics of mouse donor spermatogonial stem cell colonization in recipient testes. *Biol Reprod* 60:1429–1436.
20. Parreira GG, et al. (1998) Development of germ cell transplants in mice. *Biol Reprod* 59:1360–1370.
21. Harison DE (1980) Competitive repopulation: A new assay for long-term stem cell functional capacity. *Blood* 55:77–81.
22. Lin H, et al. (2009) Increased proliferation but decreased steroidogenic capacity in Leydig cells from mice lacking cyclin-dependent kinase inhibitor 1B. *Biol Reprod* 80:1232–1238.
23. Holsberger DR, et al. (2005) Cell-cycle inhibitors p27Kip1 and p21Cip regulate murine Sertoli cell proliferation. *Biol Reprod* 72:1429–1436.
24. Cheng T (2004) Cell cycle inhibitors in normal and tumor stem cells. *Oncogene* 23:7256–7266.
25. Kippin TE, Martens DJ, van der Kooy D (2005) p21 loss compromises the relative quiescence of forebrain stem cell proliferation leading to exhaustion of their proliferation capacity. *Genes Dev* 19:756–767.
26. Takubo K, et al. (2008) Stem cell defects in ATM-deficient undifferentiated spermatogonia through DNA damage-induced cell-cycle arrest. *Cell Stem Cell* 2:170–182.
27. Beumer TL, et al. (1999) Regulatory role of $p27^{kip1}$ in the mouse and human testis. *Endocrinoloogy* 140:1834–1840.
28. Fotovati A, Nakayama K, Nakayama KI (2006) Impaired germ cell development due to compromised cell cycle progression in Skp2-deficient mice. *Cell Div* 1:4.
29. Susaki E, Nakayama KI (2007) Multiple mechanisms for $p27^{kip1}$ translocation and degradation. *Cell Cycle* 6:3015–3020.
30. Besson A, Gurian-West M, Schmidt A, Hall A, Roberts JM (2004) $p27^{kip1}$ modulates cell migration through the regulation of RhoA activation. *Genes Dev* 18:862–876.

OPEN ACCESS Freely available online

PLoS one

Phenotypic Plasticity of Mouse Spermatogonial Stem Cells

Hiroko Morimoto[1☯], Mito Kanatsu-Shinohara[1☯], Seiji Takashima[1], Shinichiro Chuma[2], Norio Nakatsuji[2], Masanori Takehashi[1¤], Takashi Shinohara[1,3*]

1 Department of Molecular Genetics, Graduate School of Medicine, Kyoto University, Kyoto, Japan, **2** Department of Development and Differentiation, Institute for Frontier Medical Sciences, Kyoto University, Kyoto, Japan, **3** Japan Science and Technology Agency, CREST, Kyoto, Japan

Abstract

Background: Spermatogonial stem cells (SSCs) continuously undergo self-renewal division to support spermatogenesis. SSCs are thought to have a fixed phenotype, and development of a germ cell transplantation technique facilitated their characterization and prospective isolation in a deterministic manner; however, our in vitro SSC culture experiments indicated heterogeneity of cultured cells and suggested that they might not follow deterministic fate commitment in vitro.

Methodology and Principal Findings: In this study, we report phenotypic plasticity of SSCs. Although c-kit tyrosine kinase receptor (Kit) is not expressed in SSCs in vivo, it was upregulated when SSCs were cultured on laminin in vitro. Both Kit^- and Kit^+ cells in culture showed comparable levels of SSC activity after germ cell transplantation. Unlike differentiating spermatogonia that depend on Kit for survival and proliferation, Kit expressed on SSCs did not play any role in SSC self-renewal. Moreover, Kit expression on SSCs changed dynamically once proliferation began after germ cell transplantation in vivo.

Conclusions/Significance: These results indicate that SSCs can change their phenotype according to their microenvironment and stochastically express Kit. Our results also suggest that activated and non-activated SSCs show distinct phenotypes.

Citation: Morimoto H, Kanatsu-Shinohara M, Takashima S, Chuma S, Nakatsuji N, et al. (2009) Phenotypic Plasticity of Mouse Spermatogonial Stem Cells. PLoS ONE 4(11): e7909. doi:10.1371/journal.pone.0007909

Editor: Robert Feil, CNRS, France

Received August 27, 2009; **Accepted** October 19, 2009; **Published** November 19, 2009

Funding: Financial support for this research was provided by the Ministry of Education, Culture, Sports, Science, and Technology of Japan (http://www.mext.go.jp/english/), and the Japan Science and Technology Agency (CREST)(http://www.ipscc.jst.go.jp/english/index.html). The funders had no role in study design, data collection and analysis, decision to publish, or preparation of the manuscript.

Competing Interests: The authors have declared that no competing interests exist.

* E-mail: tshinoha@virus.kyoto-u.ac.jp

¤ Current address: Laboratory of Pathophysiology and Pharmacotherapeutics, Osaka Ohtani University, Tondabayashi, Osaka, Japan

☯ These authors contributed equally to this work.

Introduction

Spermatogonial stem cells (SSCs) provide the foundation for spermatogenesis throughout the life of male animals [1,2]. These cells produce differentiating cells and also maintain an undifferentiated state by undergoing self-renewal division. Despite their unique biology, the regulatory mechanism of SSC self-renewal has remained unclear. During the last decade, however, attempts have been made to characterize the surface phenotype of SSCs. Studies have established that SSCs express α6- and β1-integrin, GFRα1, CD9, Thy-1, and EpCAM but are negative for c-kit (Kit) or SSEA-1 [3]. Expression of these markers was analyzed using a germ cell transplantation technique transplanting cells freshly prepared from testes, because SSC activity, by definition, is examined only retrospectively after examining the characteristic of daughter cells [4]. These surface markers proved to be useful to purify SSCs in a deterministic manner by combining multiple parameters using cell sorter [5].

Recent studies revealed important functions of surface molecules on SSCs. For example, β1-integrins on SSCs play pivotal roles in migration into a germline niche after transplantation [6]. Another study also showed that GFRα1, which comprises a receptor for glial cell line-derived neurotrophic factor (GDNF), regulates SSC self-renewal. GDNF from Sertoli cells maintains SSCs in an undifferentiated state by binding to the GFRα1-c-ret receptor complex [7]. GFRα1 is expressed in a small population of undifferentiated spermatogonia, and changes in GDNF or GFRα1 levels can influence the fate of SSCs. For example, when GDNF is overexpressed in testes, spermatogenesis is impaired and clumps of undifferentiated spermatogonia accumulate in seminiferous tubules [7]. By contrast, a decrease in GDNF or GFRα1 level induces SSC differentiation and male infertility [7,8]. In addition to GDNF, Sertoli cells secrete another cytokine, Steel factor (Sl). Sl binds to Kit on germ cells, and a lack of Sl-Kit interaction also results in impaired spermatogenesis [9]. However, Kit is not expressed in SSCs, but it promotes proliferation and suppresses apoptosis of differentiating spermatogonia [5,9–11]. Nevertheless, the number of SSCs in Steel/Steel dickie (Sl^d) mutant mice, which lack membrane-bound Sl, is reduced to ~5% of wild-type (WT) mice. SSCs in these mice do not regenerate to the basal number,

suggesting that Sl-Kit interaction influences SSC number in Sl^d mice [12]. Thus, how environmental stimuli influence SSCs in the decision between self-renewal and differentiation via surface molecules remains unclear.

In 2003, a long-term culture system for SSCs was reported [13]. Cultured SSCs, designated as germline stem (GS) cells, continued to proliferate for more than 2 years while maintaining stable genetic and epigenetic properties [14]. Development of this culture systems provided possibilities to study SSCs in vitro. However, the percentage of SSCs in GS cell culture was unexpectedly low, and only 0.04–1.26% could colonize and reconstitute seminiferous tubules of infertile animals [15]. Moreover, a variable proportion of the cells express Kit, suggesting that a majority of GS cells are differentiating spermatogonia. In contrast, transfection experiments suggested that a significant proportion of GS cells can act as SSCs. When GS cell clones were established by electroporation with a neo-resistant gene, ~20% of picked GS cell colonies colonized seminiferous tubules and produced transgenic offspring [16]. These conflicting experiments suggest that SSC frequency is much higher than previous estimates by direct transplantation and also suggested that SSCs in vitro may exhibit properties that are distinct from those sustaining spermatogenesis in vivo.

In the present study, to clarify the phenotype of SSCs in vitro, we fractionated GS cells according to Kit expression, and examined the SSC activity using a germ cell transplantation technique. We found that GS cells show a constant level of SSC activity regardless of Kit expression. Kit was also strongly expressed in SSCs in vivo when they actively increase their number to colonize seminiferous tubules.

Results

Heterogeneity of GS Cells

We previously reported that a significant proportion of GS cells express Kit [13]. We therefore assumed that SSCs would be enriched by removing Kit^- cells from the culture, because Kit is expressed in differentiating spermatogonia. However, Kit expression in mouse embryonic fibroblast (MEF)-based GS cell culture varied depending on the timing of analysis, and we could not get consistent results. On the other hand, GS cells proliferate for long periods on laminin-coated dishes [15]. GS cells on laminin differ from those on MEFs in colony morphology. Although they form three-dimensional clump-like colonies similar to GS cells on MEFs, they can also form two-dimensional flat colonies (Figure 1A). When these cells were analyzed by flow cytometry, they were different from those on MEF in Kit expression levels (Figure 1B). Whereas the percentage of Kit-expressing cells increased up to ~90% in the flat colony, clump-type colonies showed little or no Kit expression. In both conditions, >95% of the cultured cells remained viable.

Of the several factors examined (laminin concentration, incubation time, and temperature), we found that the development of two kinds of colonies was most strongly influenced by plating density (Figure 1C). When cells were plated at 1×10^5 cells/3.8 cm^2, 60–90% of the cultured cells showed Kit expression. However, very little expression was observed when cells were plated at $<3.3\times10^4$/3.8 cm^2. Seeding density also had an impact on GS cell proliferation, and GS cells in clump-like colonies did not proliferate as much as did those in fibroblast-like colonies (Figure 1D). Consistent with this observation, Akt, which promotes GS cell proliferation [3,17,18], was strongly phosphorylated when GS cells were plated at the higher cell density (Figure 1E).

Using two different cell densities (1×10^5 and 3.3×10^4 cells/cm^2), we analyzed the expression of other cell surface markers by flow cytometry (Figure 1B). Although the two types of cells showed a significant difference in Kit expression level, GFRα1, a marker for A single (A_s) and A paired (A_{pr}) spermatogonia, and E-cadherin, a marker for undifferentiated spermatogonia [3], were expressed at comparable levels regardless of the type of colonies. We did not find significant changes in other spermatogonia or SSC markers, including α6- and β1-integrins.

Because a difference in cell shape implicated changes in cytoskeletal tension [19], we checked whether actin cytoskeleton was involved in Kit expression by adding actin-disrupting cytochalasin D. Cytochalasin D not only changed the shape of GS cells but it also decreased Kit expression (Figure 1F and G). Because small G proteins are central regulators of cell contractility, we also checked the effect of small G proteins by producing GS cells that stably express Rac, RhoA, and cdc42 dominant-negative mutants. Although no apparent morphological differences were noted among transfectants, dominant-negative RhoA mutants clearly decreased Kit expression (Figure 1F and G). These results suggested that cytoskeletal tension plays an important role in regulation of Kit expression.

Analysis of Kit Function in GS Cell Self-Renewal and Homing into Niche

Although strong Kit expression in feeder-free culture conditions suggested that the undifferentiated state of SSCs is not maintained effectively, GS cells on laminin could be maintained for 6 months without losing SSC potential [15], which raised the possibility that Kit expression was correlated with SSC activity. To examine whether Kit is necessary for GS cell proliferation on laminin, we used a Kit inhibitor (ISCK03) to study the role of Kit in GS cells on laminin. Although the inhibitor prevented proliferation of control Kit-dependent F-36P leukemic cells in a dose-dependent manner [20], it did not show any effects on GS cells (Figure 2A and B). Addition of ACK2, a Kit neutralizing antibody, also did not influence GS cell proliferation (data not shown). These results agreed with the previous observation that Kit is dispensable for proliferation of undifferentiated spermatogonia [9–11]. On the other hand, we also examined whether Kit expression can promote GS cell proliferation. Different concentrations of soluble Sl (5 to 150 ng/ml) were added to the laminin culture, but the number of cells that recovered after a 5 day-period did not show a significant increase compared with control, and they maintained their fibroblastic morphology (data not shown).

Although these results suggested that Kit is dispensable in GS cell proliferation, it was still possible that soluble Sl did not provide a strong signal through Kit; it is known that membrane-bound Sl can activate Kit more strongly [21]. Indeed, Sl^d mutant mice, which lack the membrane-bound form of Sl, are deficient for spermatogenesis despite the expression of soluble Sl [12]. To overcome this problem, we stably transfected WT Sl and dominant active Kit cDNA (Val559 to Gly mutation; Kit-G559) into GS cells derived from an enhanced green fluorescent protein (EGFP)-expressing transgenic mouse [22]. While Kit-G559-transfected cells ($GS^{Kit\text{-}G559}$) did not change morphology, Sl-transfected cells (GS^{Sl}) produced elongated colonies and did not show flat appearances despite being plated at high cell density (Figure 2C). Although Western blot showed phosphorylation of Kit in WT and the transfected GS cells, the transgenes could not replace any of the cytokines used in GS cell culture (Figure 2D).

We further examined the effect of the transgenes in SSC colonization by germ cell transplantation [4]. GS^{Sl}, $GS^{Kit\text{-}G559}$ and GS^{WT} cells were transplanted into WBB6F1-W/W^v (W) mice, which lack endogenous differentiating germ cells [11]. Two months after transplantation, numbers of colonies in recipient

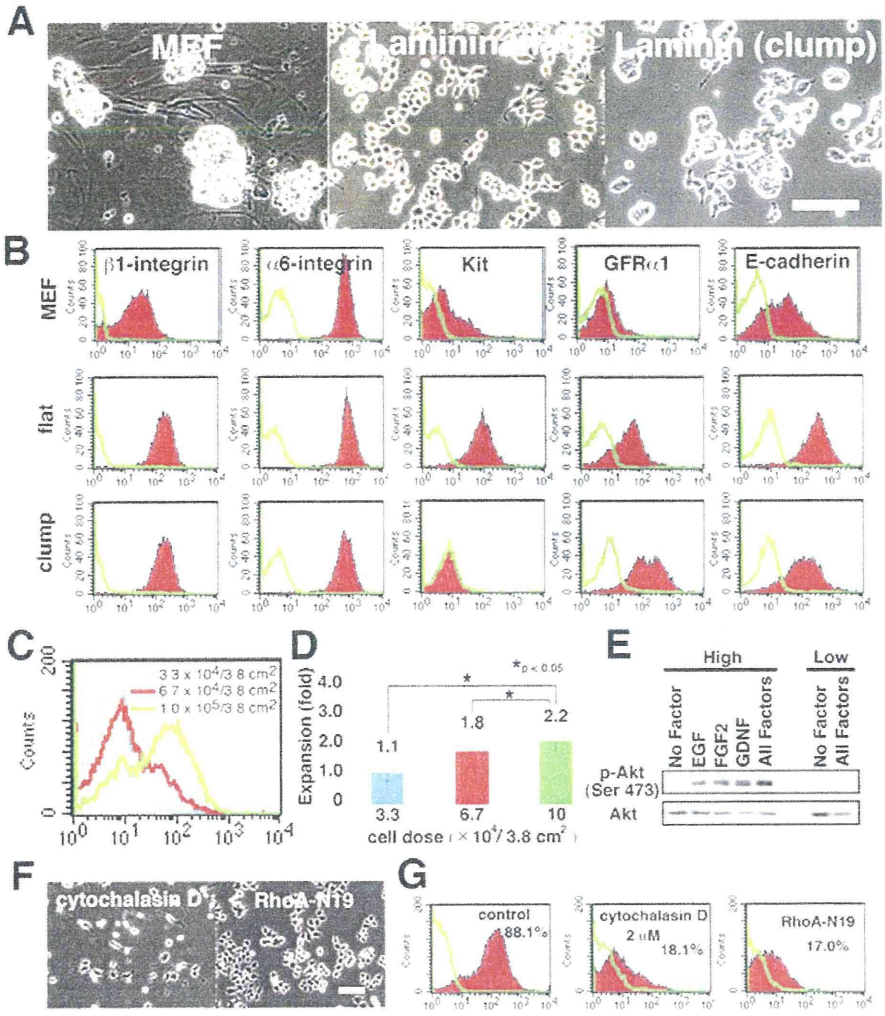

Figure 1. GS cells express Kit. (A) Morphological appearance. (B) FACS analysis of surface markers. Green line indicates the control. (C, D) Effect of cell density on Kit expression (C) and GS cell expansion (D). Cells were plated at the indicated density on laminin (n = 6). Values indicate the degree of expansion from the initially plated cells. (E) Western blot analysis of GS cells plated at 5×10^5 or 3×10^4 cells/9.5 cm^2. (F, G) Appearance (F) and Kit expression (G) of GS cells after cytochalasin D treatment or transfection of RhoA-N19 cDNA. Bar = 100 μm (A, F).
doi:10.1371/journal.pone.0007909.g001

testes were counted under UV light (Figure 2E). Although both transgenes did not influence SSC homing (Figure 2F and G), we noticed abnormalities in subsequent colony development. Interestingly, while GS^{WT} and $GS^{Kit\text{-}G559}$ could differentiate normally, GS^{SI} cells could not initiate vertical differentiation in the recipient testes (Figure 2E, inset), suggesting that regulation of Kit activation is critical for completing spermatogenesis. Thus, activation of Kit did not influence GS cell proliferation or SSC homing into the germline niche but has an impact on subsequent differentiation.

SSC Activity of GS Cells with Kit Expression

To directly test whether Kit-expressing GS cells on laminin can colonize seminiferous tubules, we used magnetic activated cell sorting (MACS) (Figure 3A). EGFP-expressing fibroblastic GS cells were selected by anti-Kit antibody, and were used for selection. After selection, 5.2±1.8% (n = 3) of the cultured cells could be recovered, and cells were then microinjected into seminiferous tubules of W mice. Two months after transplantation, analysis revealed that Kit-expressing cells have SSC activity. Whereas control unfractionated cells produced 17.2±2.4 colonies/10^4 injected cells, Kit-expressing cells showed 13.3±2.3 colonies/10^4 injected cells (n = 18). The value was not statistically significant (Figure 3B).

To extend this observation, we next used fluorescence activated cell sorting (FACS) to fractionate GS cells on laminin according to Kit expression levels (Figure 3A and C). We initially characterized sorted cells by real-time PCR for spermatogonia marker expression. Real-time PCR analysis confirmed a difference in Kit expression levels, and showed stronger expression of several SSC markers, including Pou5f1, Zbtb16, and GFRα1, in Kit^- cells (Figure 3D). Because GFRα1 is specifically expressed in A_s, and A_{pr} undifferentiated spermatogonia in vivo and, therefore, the $GFR\alpha1^-$ population did not express Kit [3], we also checked expression patterns of GFRα1 at the protein level by flow cytometry. FACS analysis of GS cells showed that GFRα1 expression is found in both Kit^- and Kit^- cells (Figure 3E).

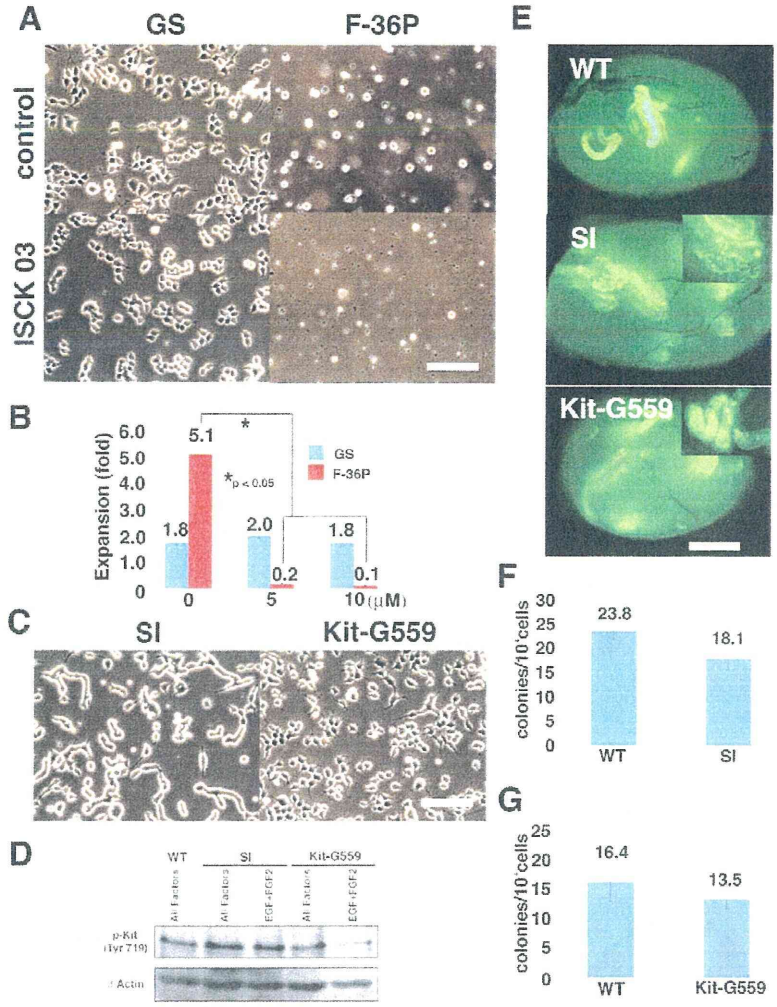

Figure 2. Dispensable role of Kit in GS cells. (A, B) Effect of Kit inhibitor (ISCK03) in colony morphology (A) and proliferation (B) of GS cells. Whereas the inhibitor could suppress the growth of the F-36P lymphocyte cell line effectively, no significant effect was found for GS cells. Cells were plated at $1\times10^5/3.8$ cm^2 and cultured with indicated cytokines for 5 (GS) or 3 (F36P) days. (C) Appearance of transfected GS cells. Note the elongated colonies of GS^{SI}. (D) Western blot analysis of transfected cells. GS^{SI} showed an enhanced phosphorylation of Kit. (E) Macroscopic appearance of recipient testes that received transfected GS cells. Whereas GS$^{Kit\text{-}G559}$ cells differentiated normally, GS^{SI} cells proliferated on the basement membrane and no vertical differentiation was observed (inset). (F, G) Homing efficiency of transfected cells. Approximately 8×10^3 cells were transplanted into each testis. No significant changes were induced by Kit-G559 (F) or SI (G) transfection. Bar = 100 μm (A, C); 1 mm (E).
doi:10.1371/journal.pone.0007909.g002

To compare proliferative potential, we cultured the sorted cells in vitro. Before initiating culture, cells from both fractions were microinjected into W mice directly to evaluate initial SSC content (Figure 3F). The remainder of the sorted cells was plated in culture for in vitro expansion. In these experiments, cells were plated on MEFs, because they promoted the survival of sorted cells more efficiently than did laminin possibly because of damage after sorting. In three sets of experiments, total cell numbers from both fractions expanded 8 to 55-fold during these 2 weeks of culture, regardless of Kit expression levels. After 2 weeks of culture, cells were transplanted into W mice to measure the increase in SSC numbers.

Analyses of recipient animals confirmed the results of MACS experiment; fresh Kit$^+$ produced 18.4 ± 1.2 colonies/10^4 injected cells ($n=14$), whereas Kit$^-$ cells yielded 16.5 ± 1.6 colonies/10^4 injected cells ($n=17$, Figure 3G). Differences between the two fractions were not statistically significant. Moreover, the concentration of SSCs in GS cell culture was also comparable after in vitro culture. Cultured Kit$^+$ and Kit$^-$ cells produced 20.0 ± 1.3 and 22.5 ± 2.2 colonies/10^4 injected cells ($n=14$), respectively. The overall increase in SSC number (SSC concentration × cell increase) in Kit$^+$ and Kit$^-$ cells was 17.5 and 16.0-fold, respectively, and the difference was not statistically significant (Figure 3H). Histological analysis confirmed normal spermatogenesis (Figure 3I). These results indicated that Kit$^+$GS cells not only had SSC activity but also underwent self-renewal division at a level comparable to Kit$^-$ GS cells.

Changes in SSC Phenotype In Vivo

Finally, we examined whether SSCs undergo phenotypic changes in vivo. We hypothesized that active proliferation of

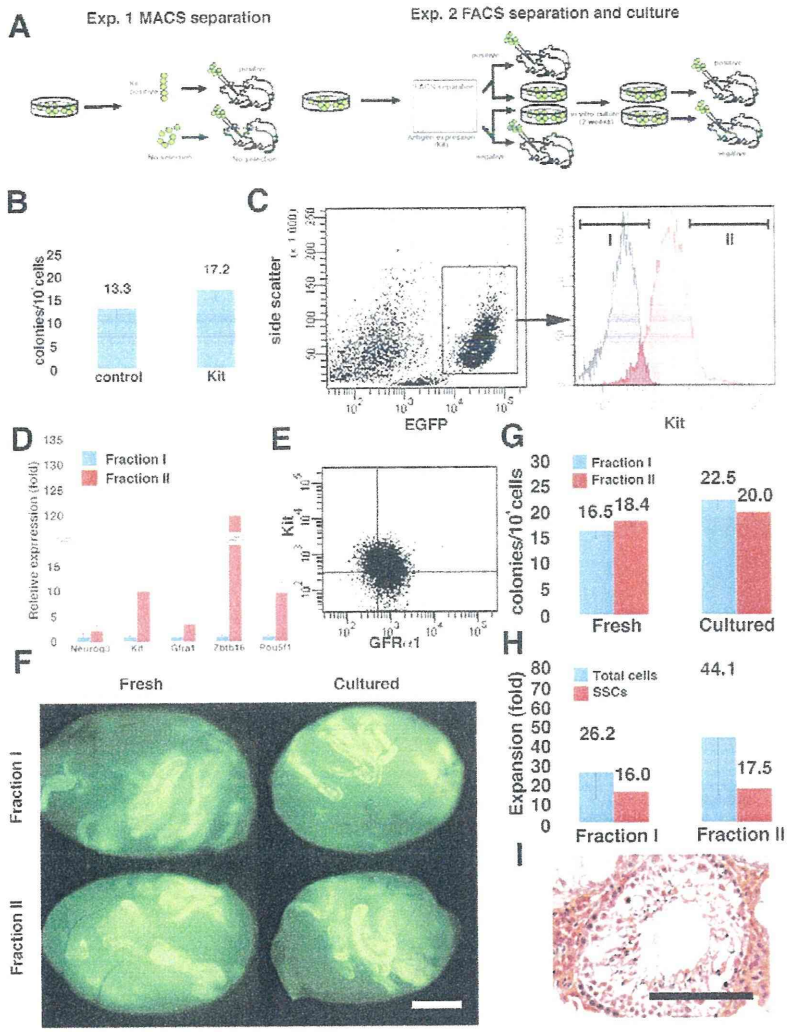

Figure 3. Fractionation of GS cells by Kit. (A) Experimental strategy. In the first experiment, Kit-expressing cells were selected by MACS. In the second experiment, GS cells were separated according to Kit expression levels by FACS. A portion of sorted cells was directly injected in each testis, and the rest of the cells were cultured for 2 weeks before transplantation. (B) SSC activity of MACS-separated cells. No significant difference was found. (C) Fractionation of GS cells by FACS. Distributions of stained (red) or control (black) are shown. (D) Real-time PCR analyses of sorted cells (n = 3–8). (E) Double immunostaining of GS cells by Kit and GFRa1. (F) Appearance of testes that received fresh and cultured cells. (G) SSC activity of fresh and cultured cells. No significant difference was found. (H) Increase in cell and SSC number after 2 weeks of culture. No significant difference was found. (I) Spermatogenesis in the recipient testis. Bar = 1 mm (F), 100 μm (I).
doi:10.1371/journal.pone.0007909.g003

SSCs might induce such changes and examined phenotypes of SSCs after germ cell transplantation. It is considered that SSCs expand in seminiferous tubules by increasing the probability of self-renewal division during the early phase of transplantation [23]. Three months after transplantation, however, transplanted cells establish a spermatogenic wave and produce spermatozoa.

We microinjected EGFP-expressing GS cells into the seminiferous tubules of W mice (primary recipients). The recipient animals were sacrificed at early (2 to 4 weeks) and late (3 to 4 months) time points after transplantation, and single cells were obtained by enzymatic digestion (Figure 4A). Expression of Kit or GFRα1 in donor cells could be specifically analyzed by gating cells with an EGFP donor marker (Figure 4B), which was downregulated during meiosis [11]. Whereas EGFP$^-$ cells showed a low side-scatter value in recipients at the early time point, they exhibited higher side-scatter value at late time point, indicating the progression of spermatogenesis [5]. Interestingly, development of this Kit$^-$ population in recipients did not depend on membrane-bound Sl, because ~20% of Kit$^-$ cells were found when GS cells were transplanted into Sl^d testes (Figure 4C–E). On the other hand, Sl^d testes were enriched with GFRα1$^-$ cells, suggesting that germ cells in Sl^d testes were relatively undifferentiated. No significant difference in β1-integrin expression was observed.

We fractionated the EGFP$^-$ donor cells in the primary W recipient mice according to Kit or GFRα1 levels by cell sorting, and cells were retransplanted into seminiferous tubules of W mice (secondary recipients) to evaluate SSC activity. The number of colonies was smaller than were those from GS cells, suggesting that SSCs undergo more predominant differentiating divisions in vivo. Nevertheless, SSC activity was found in both Kit$^-$ and Kit$^-$

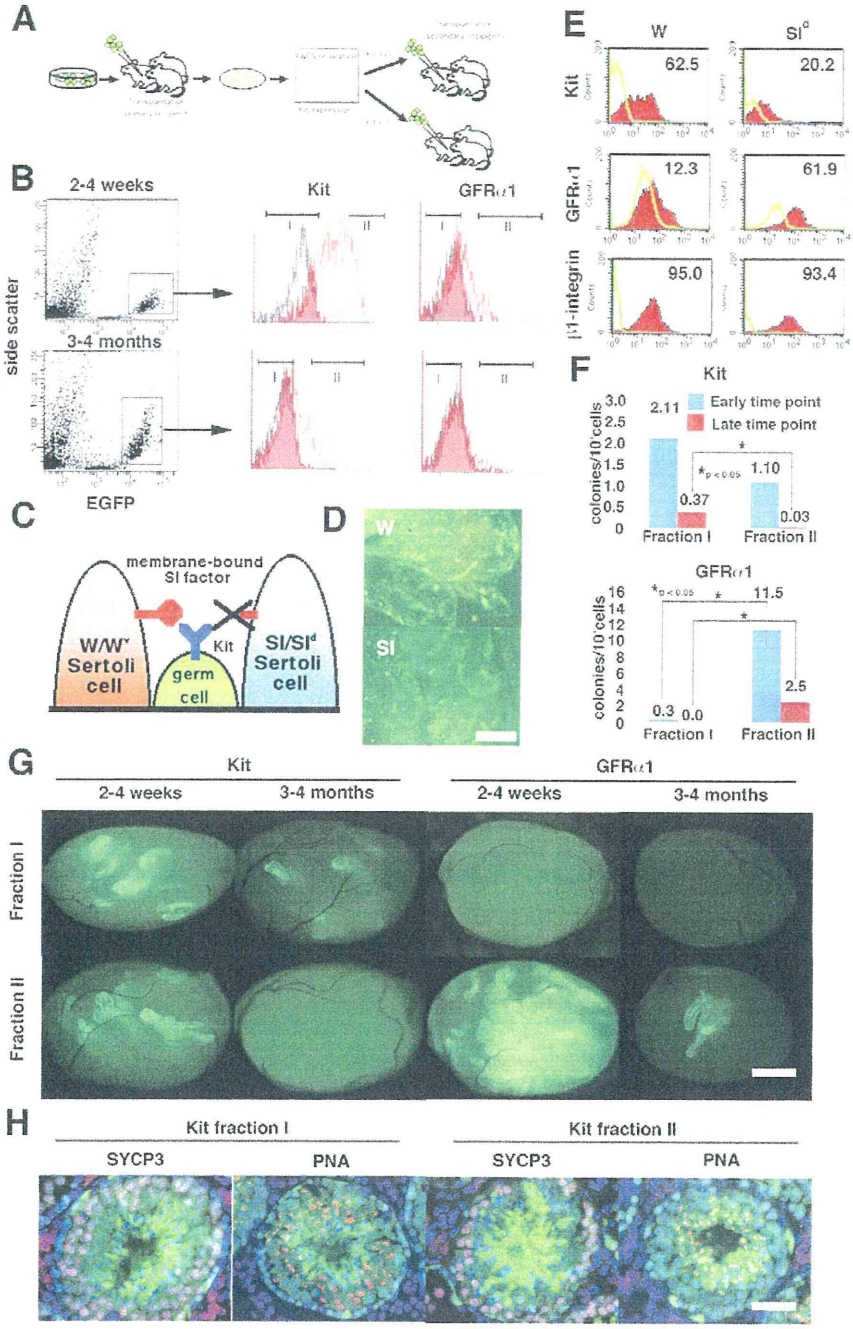

Figure 4. Changes in Kit expression in vivo. (A) Experimental strategy. After transplantation of GS cells, EGFP-expressing donor cells were fractionated according to Kit or GFRα1 levels. Sorted cells were transplanted into W mice. (B) Fractionation of donor spermatogenic cells. EGFP$^+$ cells were gated and fractionated into two groups according to Kit or GFRα1 levels. Distributions of stained (red) or control (black) are shown. (C) Sl-Kit interaction in W and Sl^d mice. Germ cells in W mice have a defect in Kit and cannot respond to Sl, whereas Sertoli cells in Sl^d mice do not express membrane-bound Sl and cannot support differentiation. (D) Appearance of W and Sl^d recipient testes 2 weeks after transplantation. Differentiation was limited in Sl^d testis. (E) FACS analysis of W and Sl^d recipient testis after transplantation. EGFP$^+$ cells were gated for analysis. (F) SSC activity of sorted cells. Both Kit$^-$ and GFRα1$^+$ cells showed significant enrichment of SSCs at both time points. (G) Appearance of recipient testes that received sorted cells. (H) Immunohistological section of the recipient testes that received Kit$^+$ or Kit$^-$ cells. The donor cells were collected from the primary recipient testes 2 weeks after transplantation, and the recipient testes were stained 2 months after cell sorting. The sections were stained with Rhodamine-PNA (red) for acrosomes and with anti-SYCP3 antibody (blue) for meiotic cells. Bar = 20 μm (D), 100 μm (G), 50 μm (H).
doi:10.1371/journal.pone.0007909.g004

fractions when sorted cells were collected from recipients that had received donor cells within 4 weeks (Figure 4F and G). The number of colonies generated was 3.45±0.64 (n = 23) and 1.07±0.19 (n = 25)/10^4 injected cells for Kit$^-$ and Kit$^-$ cells, respectively. Although the difference was statistically significant, SSCs expressing Kit were found in 5 of 6 experiments. In contrast, GFRα1$^-$ cells were significantly enriched for SSCs, and results from three experiments showed that the numbers of colonies were 0.3±0.1 and 11.5±2.0/10^4 injected cells (n = 15) for GFRα1$^+$ and GFRα1$^-$ cells, respectively (Figure 4F and G).

When sorted cells were collected from primary recipients between 3 and 4 months after transplantation, results from two experiments showed that the difference in SSC activity became more pronounced and the average numbers of colonies were 0.37±0.08 (n = 8) and 0.03±0.03 (n = 10)/10^4 injected cells for Kit$^-$ and Kit$^-$ cells, respectively. In contrast, SSCs were consistently positive for GFRα1, and 2.5±1.0 colonies/10^4 injected cells (n = 10) were generated only from GFRα1$^-$ cells. Immunohistological staining of the recipient testes showed normal spermatogenesis from both Kit$^+$ and Kit$^-$ cells. No significant differences in SYCP3 (meiotic cell marker) or PNA (acrosome marker) expression patterns were observed (Figure 4H). These results show that SSCs also change Kit expression levels during regeneration in vivo.

Discussion

Although both phenotypic and functional analyses suggested that most GS cells are progenitors without SSC activity, single-cell cloning experiments in our previous study showed that a significant proportion of GS cells maintain a potential to function as SSCs [16]. The current study was initiated to resolve the discrepancy between these findings, and we provide evidence that SSCs change their phenotype according to their microenvironment. Our conclusion was supported by our two transplantation experiments. First, in GS cell culture, Kit$^-$ cells proliferated as actively as Kit$^+$ cells and frequency of SSCs was comparable between the two populations. Second, immediately after transplantation, we found weaker but distinct SSC activity in the Kit$^-$ donor cell population. These findings contrast with previous observations that SSCs do not express Kit. They also suggest that SSCs in vitro probably do not follow traditional scheme of SSC self-renewal [1,2].

One of the important factors that contributed to phenotypic changes was laminin. Several lines of evidence have suggested that laminin plays critical roles in SSC biology. First, SSCs express both α6- and β1-integrin strongly and preferentially attach to laminin compared with other extracellular matrix substrates in vitro [12]. Second, β1-integrin-deficient SSCs that failed to attach to laminin could not settle in the germline niche [6]. Third, SSCs from mice, rats and hamsters all proliferate on laminin for several months without losing germline potential, suggesting that the ability to bind to laminin is beneficial and conserved among species [15,24,25]. Therefore, we speculated that integrin-laminin interactions in vitro might partly mimic stem cell-niche interactions in vivo, and assumed that culturing on laminin would create a more hospitable environment for SSCs. Given these results, we did not expect that GS cells on laminin would strongly upregulate Kit, a marker of differentiating spermatogonia.

Another factor that influenced SSC phenotype was plating density. Cell density or shape has been shown to influence many biological processes, including the lineage-specific marker expression or differentiation of stem cells. For example, changes in mechanical tension mediated by RhoA-ROCK signaling pathway regulated the fate commitment of mesenchymal stem cells (MSC)[19]. Dominant-negative RhoA committed MSCs to become adipocytes, whereas constitutive-active RhoA caused osteogenesis. Low plating density also enhanced their proliferation. In contrast, GS cells proliferated more slowly at low density, but cytochalasin D or transfection with dominant-negative RhoA reduced Kit expression, suggesting the involvement of actin cytoskeleton in Kit expression. This finding suggests the importance of cell structure and mechanics in the modulation of SSC phenotype and heterogeneity.

Our retransplantation experiments showed that SSCs also change their phenotype in vivo. Retransplantation is a unique model to study SSC regeneration, because it allows SSCs to increase their number in vivo [26]. In normal testes, SSCs are kept under constant pressure to differentiate to produce sperm. SSCs undergo only two types of cell division, and they produce either two stem cells or two progenitor cells [1,2]. However, the concentration of GDNF in the Sl^d or W testis is upregulated by a deficiency of endogenous germ cells [27], and this probably promoted transplanted SSCs to preferentially undergo symmetric self-renewal divisions to fill empty niches. Indeed, undifferentiated spermatogonia in Sl^d mice take up BrdU more rapidly than those in WT mice [27]. However, as SSCs gradually repopulate to establish normal cycles of spermatogenesis with time, the probability of self-renewing division progressively decreases by downregulation of GDNF and they no longer exhibit an activated phenotype. On the other hand, in other models used to study SSC regeneration, such as experimental cryptorchidism or vitamin A deficiency [5,10], the number of SSCs remains constant, and this may explain why these treatments could not induce Kit in undifferentiated spermatogonia. Based on these observations, we suggest that, when SSCs are relieved from steady state kinetics, such as after germ cell transplantation or in vitro culture, they may be exempted from required differentiation and are induced to express Kit (Figure 5).

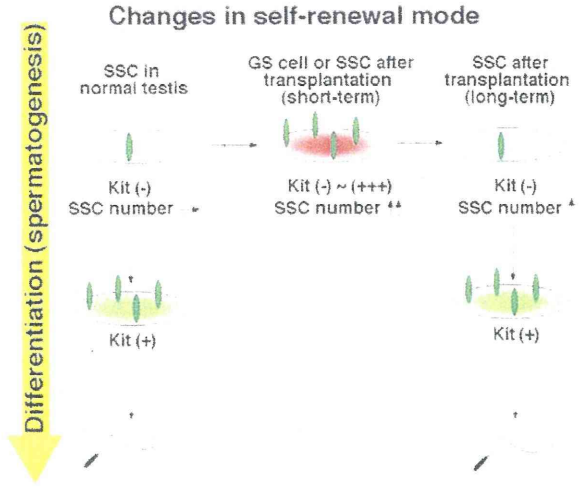

Figure 5. Expression of Kit on SSCs during active proliferation. SSCs in normal testes do not express Kit and maintain a constant number (non-activated state). However, when SSCs increase their number during culture or soon after transplantation, they upregulate Kit (activated state). Kit is downregulated in SSCs when germ cell colonies resume normal spermatogenesis.
doi:10.1371/journal.pone.0007909.g005